To the Graduate Council:

I am submitting herewith a dissertation written by Christine Leigh Copper entitled "Mechanistic and Molecular Modeling Studies of Several Capillary Electrophoretic Separation Techniques Employing Cyclodextrin Additives." I have examined the final copy of this dissertation for form and content and recommend that it be accepted in partial fulfillment of the requirements for the degree of Doctor of Philosophy, with a major in Chemistry.

Michael J. Sepaniak, Major Professor

We have read this dissertation
and recommend its acceptance:

Accepted for the Council:

Associate Vice Chancellor and
Dean of The Graduate School

Mechanistic and Molecular Modeling Studies of Several Capillary Electrophoretic Separation Techniques Employing Cyclodextrin Additives

A Dissertation

Presented for the Doctor of Philosophy

Degree

The University of Tennessee, Knoxville

Christine Leigh Copper

August 1995

Dedication

To my brothers, Tom and Doug, who made me tough enough to handle anything, even graduate school.

Acknowledgements

I would not be completing my graduate degree if it were not for the help and encouragement of several individuals. Most importantly, I am grateful for the direction given to me by Mike Sepaniak. Without his input and his patience, not to mention his research grants, this work would not have been possible.

Thanks also go to my parents, Walter and Barbara Copper, for teaching me that a little determination makes anything possible. I also thank them for providing me with enjoyable homes to visit when times got tough.

I am appreciative of the guidance (and tennis matches) provided by the members of my committee: Georges Guiochon, David Baker, and Walker Smith.

Finally, I wish to acknowledge the friends that made graduate school a memorable experience. I sincerely thank Lenni and Julie, who probably now need counseling, for dealing with me for several years. Thanks also to Carlos and Nicole, Roy, Bob, the "tennis ladies," Steve, Lu, and the Sepaniak group members that I have worked with throughout my graduate studies.

Abstract

Important historical and theoretical concepts of capillary electrophoretic separations are presented as a basis for understanding the three capillary electrophoretic techniques described. The influence of several fundamental parameters on separation performance in each of the techniques is discussed. In most cases, efficiency, selectivity, and system retention are found to be most important in defining separation mechanisms. Molecular modeling is used to study interactions between solutes and cyclodextrin separation buffer additives to gain further information regarding separation mechanisms.

The resolving power of combinations of cyclodextrins and surfactants is demonstrated by cyclodextrin-modified micellar electrophoretic capillary separations of highly hydrophobic polycyclic aromatic hydrocarbons. These separations are optimized by altering the type and concentration of cyclodextrin, surfactant and organic modifier. Correlations are drawn between the elution order of several substituted benzopyrene isomers and computationally derived interaction energies.

Enantiomers of several dansyl amino acids and binaphthyl compounds are resolved in separate studies using cyclodextrin-modified capillary electrophoresis. Once again, correlations are found between separation behavior and molecular modeling data. Furthermore, it is shown that there is a unique optimum

cyclodextrin concentration that leads to maximum resolution of each pair of enantiomers.

A new technique, cyclodextrin distribution capillary electrochromatography, that involves the use of combinations of neutral and charged cyclodextrins is presented. Polycyclic aromatic hydrocarbons are the solutes used to evaluate the fundamental characteristics of the technique. Unique selectivities afforded by this technique lead to speculation of future capillary electrophoretic studies employing cyclodextrin additives.

Table of Contents

List of Tables

List of Figures

List of Abbreviations

ACN	acetonitrile
Asp	aspartic acid
BaP	benzo(a)pyrene
BeP	benzo(e)pyrene
BN	binaphthyl
CD	cyclodextrin
CDCE	cyclodextrin distribution capillary electrochromatography
CD-CE	cyclodextrin-modified capillary electrophoresis
CD-MECC	cyclodextrin-modified micellar electrokinetic capillary chromatography
CE	capillary electrophoresis
CM	carboxymethyl
cmc	critical micelle concentration
DNS	5-Dimethylamino-1-naphthalene sulfonyl
GC	gas chromatography
Glu	glutamic acid
HP	hydroxypropyl
HPLC	high performance liquid chromatography
i.d.	inner diameter
LC	liquid chromatography

Leu	leucine
Me	methyl
MeOH	methanol
NaC	sodium cholate
PAH	polycyclic aromatic hydrocarbon
PMT	photomultiplier tube
SDS	sodium dodecyl sulfate
Ser	serine
SPL	SYBYL programming language
THF	tetrahydrofuran
Thr	threonine
Val	valine

Chapter 1
Introduction and Organization

Chromatography

Separation is the cornerstone of many areas of chemistry. Quite often, the goal of a chemical experiment is to isolate and analyze a particular compound. Chromatography is unquestionably the most widely used method of separation in the field of analytical chemistry. It is for this reason that several classes of chromatographic techniques have been created. Crudely, these can be divided into two categories based upon the type of mobile phase employed: gas chromatography and liquid chromatography.

Gas chromatographic (GC) separations are based upon distribution of a solute between a moving, inert, carrier gas and either a solid or liquid stationary phase. GC, when compared to other chromatographic techniques, provides the best resolving power and sensitivity for volatile organic compounds. Other advantages of this technique include speed, qualitative and quantitative analysis possibilities, and instrumental simplicity (1, 2).

Compounds suitable for GC analyses must be thermally stable at the temperature required for volatilization. Typically, a molecular weight limit of 1000 and temperature limit of 400 °C govern whether or not GC is a suitable method of analysis for a particular solute (1). Many times, compounds having a molecular weight above this limit are of interest so an alternative to GC, such

as a liquid chromatographic (LC) method, is required.

LC techniques all involve a liquid mobile phase and either a solid (adsorptive or bonded phase) or liquid stationary phase, the former finding much more utility. LC methods, mainly high performance liquid chromatography (HPLC), are used in place of GC when solutes to be analyzed are nonvolatile or thermally labile. LC provides a moderate number of theoretical plates, as compared to GC but does offer advantages of ease of sample recovery, choice of detection schemes, and applicability to a wider molecular weight range of compounds (2, 3).

One important niche of LC separations is filled by capillary electrophoresis (CE). Separation in CE is based on differences in solute mobilities when an electric field is applied across the separation buffer. Compared to conventional LC techniques, CE has advantages of high efficiency, short analysis time, simple apparatus, small sample and separation buffer volumes, and ease in changing separation buffer (4). Additionally, selectivity in CE separations can be easily altered through the use of various separation buffer additives. CE employing cyclodextrin (CD) additives has been shown to provide unique selectivities when compared to other variations of CE. However, CE techniques that employ CDs, such as CD-modified micellar electrokinetic capillary chromatography (CD-MECC), CD-modified CE (CD-CE), and CD distribution capillary electrochromatography (CDCE), are relatively new. For this reason, many reports in the literature demonstrate the use of CDs in CE to separate structurally similar compounds but

present only limited discussions as to the mechanisms by which separation occurs.

Statement of Purpose

The main purpose of the research described in this document was to determine the experimental parameters that most strongly influenced CE separation performance when CDs were incorporated in the separation buffer. Once these parameters were identified, they were manipulated in attempts to define the mechanisms behind these separations. Parameters such as efficiency, resolution, selectivity and system retention were probed extensively in studies of separations of chiral and non-chiral solute molecules. The information gleaned from these separations was augmented with solute/CD interaction energies calculated via molecular modeling. In most cases, informative correlations between separation and modeling data were drawn. In some studies, solute/CD complexation constants, calculated from plots of CD concentration versus solute mobility, provided further insight into the mechanisms by which successful separation was achieved.

The solute molecules chosen for the work described in this dissertation included highly hydrophobic, polycyclic aromatic hydrocarbons (PAHs), chiral dansyl (DNS) amino acids, and chiral binaphthyl (BN) compounds. It was advantageous to study PAHs for two reasons. First, these compounds are quite rigid and relatively non-reactive. Second, they exist in many sizes (i.e., 2, 3, 4, 5 benzene rings per molecule) with isomers of each size easily

available. The two types of chiral compounds studied were chosen as test solutes because of the nature of their chirality. The DNS-amino acids each contain an asymmetric carbon while the chirality in the BN molecules is due to rotational hindrance at a 1-1' bond between two naphthalene rings in these compounds.

Organization

The remaining sections of this dissertation are organized in the following manner. In Chapter 2, the reader is introduced to the history and theory of CE. Next, a detailed description of two classes of separation buffer additives, surfactants and CDs, is presented. Chapter 3 describes the main concepts of molecular modeling. This discussion is necessary because molecular modeling studies were performed to help understand the separation behavior observed. A detailed account of all separation and molecular modeling experimental particulars comprises Chapter 4.

The foundation provided in Chapters 2, 3, and 4 allows the reader to easily assimilate the results and explanations presented in Chapters 5 through 9. Finally, some general concluding remarks, an inclusive list of references, and an appendix containing structural representations of all compounds studied make up the final sections of this document.

Chapter 2
Historical and Theoretical Aspects of Capillary Electrophoresis

Capillary Electrophoresis History

CE, in its present state, has evolved from what now seem to be rudimentary column electrophoresis techniques that were first introduced three decades ago. These early reports, many of which were made by Hjerten and Catsimpoolas, employed columns having inner diameters (i.d.s) on the mm scale (5, 6). However, advantages of smaller diameter columns were soon discovered by Virtanen (7) and by Mikkers, Everaerts, and Verheggen (8). Virtanen used Pyrex tubing with i.d.s ranging from 200 to 500 μm to quantitatively analyze Li^+, Na^+, and K^+ cations using potentiometric detection. Noteworthy in this report is his recognition of the importance of the influence of electroosmotic flow on a solute's behavior. Mikkers et al. separated a number of inorganic and organic anions using 200 μm i.d. Teflon tubing and ultraviolet and conductometric detection.

In 1981, Jorgenson and Lukacs performed the first electrophoretic separations in narrow, glass capillaries (<100 μm i.d.) (9). They separated DNS and fluorescamine derivatives of several amino acids and used fluorescence as the detection method. For reasons that will be discussed later, they were able to apply large voltages across the column to achieve very high efficiencies. Most importantly, they described some of the main concepts of CE including requirements for achieving high efficiency, the importance

of electroosmosis, and they also presented equations related to the observed separation processes.

Main Theoretical Concepts in Capillary Electrophoresis

Although the theoretical aspects of CE have be studied extensively in the time since Jorgenson and Lukac's initial report, only broad explanations of these ideas are presented in this document. Namely, topics of electroosmotic flow, solute mobility, resolution, and efficiency are addressed in the paragraphs that follow.

electroosmotic flow

Electroosmotic flow, although not entirely understood even to this day, strongly influences CE separations. Simplistically, it is the movement of solvent (i.e., separation buffer) through a silica capillary due to the existence of a zeta potential at the solvent/silica interface (i.e., capillary wall). At this interface, there exists an excess of negative charge from the deprotonated silanol groups of the capillary wall. This negatively charged surface attracts cations from the separation buffer which form an electric double layer. This layer consists of an inner layer of tightly bound, immobile ions and a diffuse outer layer of more mobile ions. Upon application of an electric field, the outer layer of cations flows towards the cathode and in the process, transports the bulk liquid in that same direction. The velocity of this electroosmotic flow (v_{eo}) can be calculated using the equation:

$$v_{eo} = \frac{\varepsilon}{4 \pi \eta} \zeta E \qquad [1]$$

where ε is the dielectric constant of the buffer, η is the buffer viscosity, E is the applied electric field, and ζ is the zeta potential (4, 10).

The magnitude of v_{eo} can be influenced in many ways. The rate of electroosmotic flow can be altered using methods such as buffer pH and/or viscosity adjustments, radial field application, addition of surfactants below their critical micelle concentration (cmc) (defined as the concentration at which micelles are formed through aggregation of surfactant monomers), and addition of organic solvents to the separation buffer (see discussions in Chapters 5, 6, and 9). In the most extreme case, electroosmotic flow can be eliminated by coating the capillary walls with reagents that result in a neutral wall coating (10).

Since electroosmotic flow is driven by the zeta potential at the capillary walls, there is a flat velocity distribution across the diameter of the capillary. This plug-like profile distinguishes CE from other column liquid chromatographic methods in which the profile is parabolic in nature. The plug-like profile of CE is advantageous because it greatly reduces the velocity gradient across the column thus reducing band broadening due to slow mass transfer across such a gradient (4).

solute mobility

The mobility (μ) of a solute in CE is dependent on a number of factors as seen in the equation:

$$\mu = \frac{q}{6\pi\eta r} \qquad [2]$$

where q is the charge of an ionic solute, η is the viscosity of the buffer, and r is the size of the molecule (related to the radius of a spherical molecule). From this equation, it can be said that a solute's mobility is directly proportional to its charge and inversely proportional to its size and the viscosity of the separation buffer (10).

Experimentally, an anionic solute's mobility is calculated using the equation:

$$\mu = \frac{L\,L_{tot}}{V} \cdot \left[\frac{1}{t_o} - \frac{1}{t_r}\right] \qquad [3]$$

where L is the distance between the point of injection and the point of detection, L_{tot} is the total length of the separation capillary, V is the applied voltage, t_o is the retention time of an unretained solute (thus a measure of electroosmotic flow), and t_r is the retention time of the solute.

resolution

The mobilities of a pair of injected solutes have a strong influence on the resolution observed between them. This is seen in the equation for resolution (R_s):

$$R_s = \frac{N^{1/2}}{4} \cdot \frac{(\mu_1 - \mu_2)}{(\mu_{ave} + \mu_{eo})} \qquad [4]$$

where N is the number of theoretical plates (see below), μ_1 and μ_2 are the mobilities of two solutes and μ_{ave} is their average mobility, and μ_{eo} is the electroosmotic mobility of the buffer system employed. Resolution is maximized by large differences in solute mobilities, high applied voltages, and electroosmotic flow opposing the mobilities of the solutes. However, extreme magnitudes of these variables can lead to problems such as long analysis times and Joule heating (11).

Joule heat is a concern in all CE separations. It is the heat generated as a result of electric current passing through the buffer solution in the separation capillary. Joule heat is dissipated at the wall of the column. As a result, the solution in the center of the column can have a higher temperature than that adjacent to the walls. Such a temperature gradient alters the buffer viscosity which leads to different solute mobilities (see Equation [2]) across the diameter of the capillary. This distribution of mobilities results in band broadening thus reducing the efficiency of the

separation (4). A temperature difference between the capillary center and wall as small as 5 °C has been shown to cause significant band broadening (10).

The amount of Joule heat generated during CE separations can be controlled by reducing the applied voltage and/or utilizing smaller diameter capillaries that exhibit lower current and, furthermore, can more effectively dissipate Joule heat.

efficiency

Under ideal conditions, axial diffusion is the primary band broadening mechanism. However, when separation buffer additives are employed, as was the case in the work described in this document, mass transfer effects can also influence separation efficiency. Efficiency, N, assuming axial diffusion dominates, is calculated using the equation:

$$N = \frac{(\mu + \mu_{eo})\, V}{2D} \qquad [5]$$

where μ is the mobility of a solute, μ_{eo} is the electroosmotic mobility of the buffer, V is the applied voltage, and D is the diffusion coefficient of the solute (10).

Efficiency is most strongly influenced by the magnitude of the voltage applied across the capillary. For this reason, high applied voltages should result in high efficiencies but at some point, the

problems associated with Joule heating (see discussion above) actually diminish the efficiency observed. Efficiency can also be limited by the concentration of solute injected, solute/wall interactions, and temperature gradients.

Accomplishments in Capillary Electrophoresis

CE has grown exponentially since the publication of the initial reports described at the beginning of this chapter. One most recent indication of this growth is the creation of a journal, *Journal of Capillary Electrophoresis*, solely dedicated to this technique. Further evidence of the expanse of CE is found in the number of review articles that have appeared in various respected journals in recent years, including *Analytical Chemistry*, *Journal of Chromatography*, and *Electrophoresis*. Reports such as these highlight the most significant developments in CE. Most of these developments can be grouped into categories of theoretical studies, column technology, detection methods, and applications (many of which involve the use of separation buffer additives) (12-17).

Because detailed information regarding each of these developments is easily accessible in the literature, it is not appropriate to address each of them in this document. However, developments in CE applications involving separation buffer additives are relevant to the research described in the chapters that follow and will therefore be discussed in some detail.

Additives in Capillary Electrophoretic Separations

Unique selectivities have been demonstrated in CE separations through the use of a wide variety of separation buffer additives. Representative examples of such additives are organic solvents (18), soluble polymers (19), surfactants (20), and neutral and charged CDs (21, 22). Enantiomeric resolution in CE has been provided by additives such as chiral surfactants, especially bile salts (23, 24), CDs (14-16, 25, 26), optically active metal complexes (27), crown ethers (28), macrocyclic antibiotics (29), and proteins (30).

Of the additives listed above, a large research effort, including the work discussed in this document, has been focused on the utilization of surfactants and CDs as separation buffer components in CE. These two classes of chemicals have been employed separately and in combination to provide resolution (enantiomeric or otherwise) in CE separations of a wide variety of solutes.

Surfactants are frequently added to CE separation buffers to separate neutral compounds. Surfactants contain both hydrophilic and hydrophobic entities. They can be anions, cations, zwitterions, or even polar neutral molecules. Most surfactants contain a polar and/or ionic head group and a nonpolar hydrocarbon tail (20).

When employed at concentrations above the cmc, surfactant monomers will aggregate to form assemblies known as micelles. Normal micelles are formed when the hydrophobic tails point inward and the polar head groups become the surface of these aggregates. When micelles are used in CE separations, the technique is sometimes dubbed micellar electrokinetic chromatography (MEKC)

(31). However, a more accurate name for this technique, which will be used in the remainder of this report, is micellar electrokinetic capillary chromatography (MECC) (32).

MECC was first reported by Terabe et al. in 1984 when they separated several phenol derivatives using a sodium dodecyl sulfate (SDS) micellar system (33). In this system, which is typical of all other MECC systems, the micelles represent a secondary phase and have a mobility that is a combination of their intrinsic electrophoretic mobility and the electroosmotic flow of the mobile phase. In cases where negatively charged surfactants, such as SDS are utilized, the mobility of the micelles is opposite to the electroosmotic flow. However, this mobility is overcome by the stronger electroosmotic flow and the micellar phase is ultimately transported in the same direction as electroosmotic flow. The result of these unequal mobilities is a two phase system, depicted in Figure 1, comprised of a electrophoretically transported mobile phase and an electrophoretically retarded micellar phase (20).

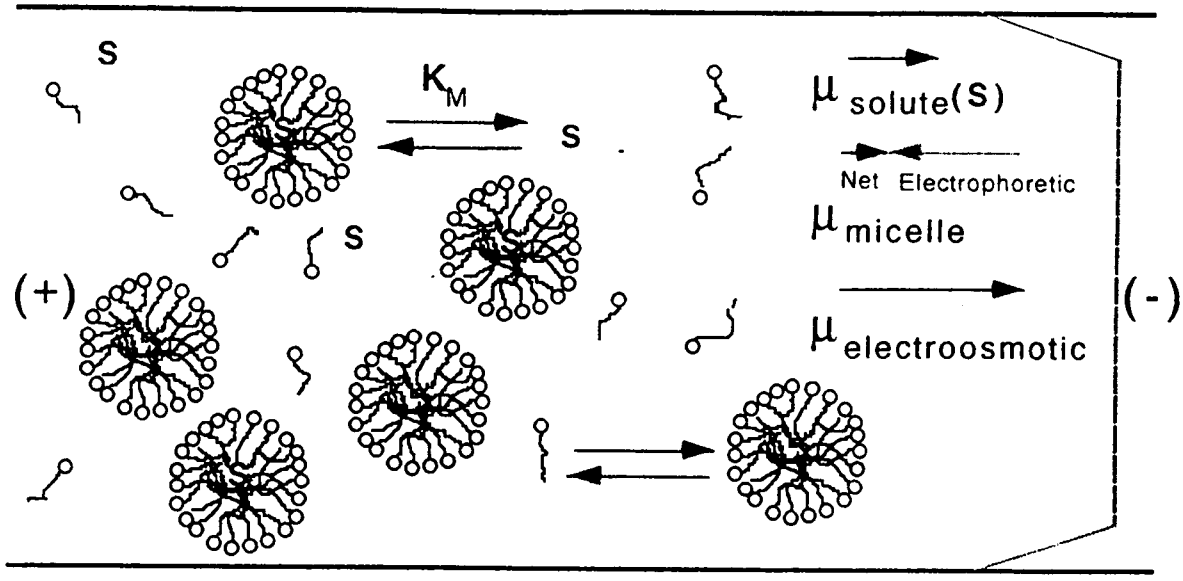

Figure 1 Depiction of flow dynamics in MECC.

Main Theoretical Concepts in Micellar Electrokinetic Capillary Chromatography

resolution

Resolution in MECC is defined by the following expression:

$$R_s = \frac{N^{1/2}}{4} \cdot \frac{\alpha - 1}{\alpha} \cdot \frac{k_2'}{1 + k_2'} \cdot \frac{1 - t_o/t_m}{1 + (t_o/t_m)k_1'} \qquad [6]$$

The four terms in Equation [6] are efficiency (measured by plate number, N), selectivity factor (α, which is the ratio of k'_1/k'_2), retention (given by capacity factors, k'_1 and k'_2 for two solutes), and the elution range (bordered by t_o and t_m) (20).

efficiency

Efficiency in MECC separations is mainly determined by mass transfer effects, micelle polydispersity, and thermal effects (20).

The plug-like velocity profile and the small size and uniform distribution of micelles act to reduce resistance to mass transfer in MECC. In addition, slow electroosmotic flow and large solute diffusion coefficients are also factors that reduce band broadening due to mass transfer effects.

Micelle polydispersity also influences efficiency in MECC. At any given time, there exist micelles of a variety of shapes and sizes in an MECC mobile phase. Since micellar mobility is dependent upon

the size and shape of the micelles, there is a range of mobilities within the micellar phase that can be experienced by a solute molecule (20). This mobility range is a source of band broadening but it can be controlled by adjusting surfactant concentration and/or operating temperature. Increasing the surfactant, thus micellar, concentration acts to compensate for the polydispersity. High surfactant concentrations, as well as increased operating temperature, increase the rate of monomer/micelle exchange. This acts to average out the effects of different micelle sizes available to a solute thus reducing band broadening due to polydispersity (20).

Efficiency in MECC can also be limited by dispersion resulting from thermal gradients within the capillary. Joule heating (see above) can be an even greater problem in MECC than it is in CE since the ionic strengths of most MECC mobile phases are greater than those used in CE.

selectivity

The second term in Equation [6] highlights the importance of selectivity factor ($\alpha = k'_1/k'_2$) in providing adequate resolution in MECC. One of the distinct advantages of MECC is the ease in which resolution can be manipulated through simple adjustment of the composition of the mobile phase (20). Both the primary (separation buffer) and secondary (micellar) phases can be rapidly changed to provide dramatic or subtle changes in selectivity. In a portion of this work, different types of surfactants, organic modifiers, and CDs

have been employed in MECC mobile phases to provide desired selectivity (see Chapters 5 and 6).

elution range/retention

The final two terms in Equation [6] relate resolution to the elution range (indicated in the final parenthetical expression) and retention (as given by k') (20).

As t_o/t_m approaches zero (indicating an infinite elution range), resolution increases, but at the expense of analysis time. A broad elution range is essential to attaining the high peak capacities required to accommodate the separation of complex mixtures. For this reason, organic modifiers are sometimes employed to extend the MECC elution range (see Chapter 5) (18).

The breadth of the elution range influences the k' value of a solute having a retention time of t_r, as seen in the equation:

$$k' = \frac{t_r - t_o}{t_o\,(1 - t_r/t_m)} \qquad [7]$$

It is important to note that values of k' are often reported as approximate due to difficulties in accurately determining t_m. Further details regarding retention in MECC and examples of k' optimization are found in Chapters 5 and 6.

Cyclodextrins in Capillary Electrophoresis

As mentioned above, CDs can be added to a CE or MECC separation buffer to effect the selectivity of the separation. CDs are a product of the enzymatic digestion of starch. They have the shape of a trunkated cone with a hydrophobic cavity and a hydrophilic exterior. The most common CDs, which are depicted in Figure 2, are comprised of six (α-CD), seven (β-CD), or eight (γ-CD) glucopyranose units. There is considerable discrepancy in the literature with regard to cavity dimensions. However, cavity diameters of ~5.0 Å, ~6.3 Å, and ~8.0 Å for α-, β-, and γ-CD, respectively, are commonly quoted (34-36). Inclusion complex formation between solutes and the CD's cavity is dependent upon the geometry, size, and physiochemical properties of the solutes. Hydrophobic interactions predominate in the cavity. However, these interactions can act in concert with polar or hydrogen bonding interactions that occur with hydroxyl groups located on the outer lip of the CD cavity. Modified CDs (including neutral and ionizable derivatives) have also been used as separation buffer additives. Moreover, the chiral nature of native and derivatized CDs provides discrimination in separations of many optical isomers (14-16, 25, 26).

In the chapters that follow, three distinctly different types of electrophoretic separation systems employing CDs are described. Briefly, these are CD-MECC (Chapters 5 and 6), CD-CE (Chapters 7 and 8), and CDCE (Chapter 9).

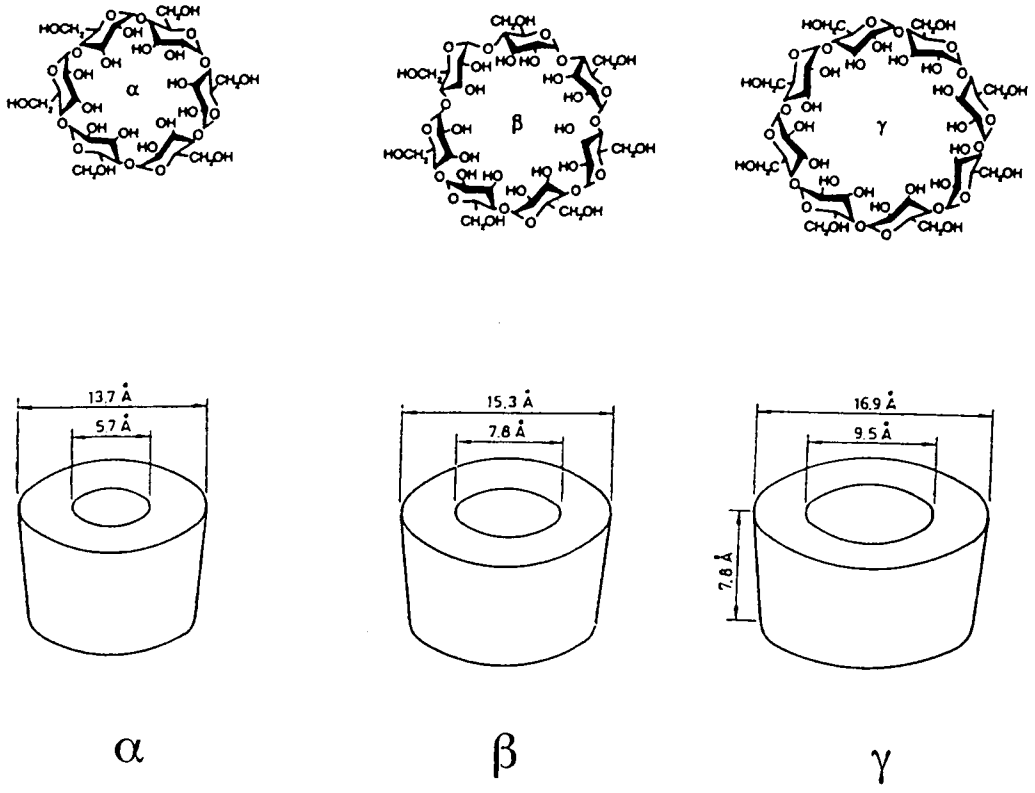

Figure 2 Depictions and dimensions of three native CDs.

In CD-MECC, neutral CDs are added to the MECC mobile phase to selectively reduce k', relative to simple MECC, due to inclusion with the CD. Since the CDs have no charge, therefore no intrinsic mobility, they travel at the electroosmotic velocity of the mobile phase. This results in a three phase system in which the mobile phase and CD phase are moving at the rate of electroosmotic flow and the electrophoretically retarded micellar system travels at a slower rate. Unequal partitioning of neutral solutes amongst these phases results in separation. CD-MECC is especially powerful in separations of highly hydrophobic compounds (such as PAHs) which tend to totally associate with the micellar phase, thus co-eluting at t_m, in unmodified MECC.

CD-CE is used to separate solutes that are ionized at the pH of the separation buffer. Generally, charged solutes can be separated in unmodified CE since their intrinsic mobilities are quite different. However, some charged solutes have similar mobilities which makes resolution difficult. In these cases, CDs are added to the separation buffer to alter selected solutes' mobilities through inclusion complex formation. Furthermore, as evidenced in some of the research described in this document, CDs can be employed as chiral selectors in a CD-CE separation buffer.

Combinations of charged and neutral CDs are added to the separation buffer in CDCE to separate neutral compounds. The combination of these two types of CDs results in a system that behaves similarly to CD-MECC as there are three phases moving at two different velocities (see Figure 3). However, in CDCE, the CD

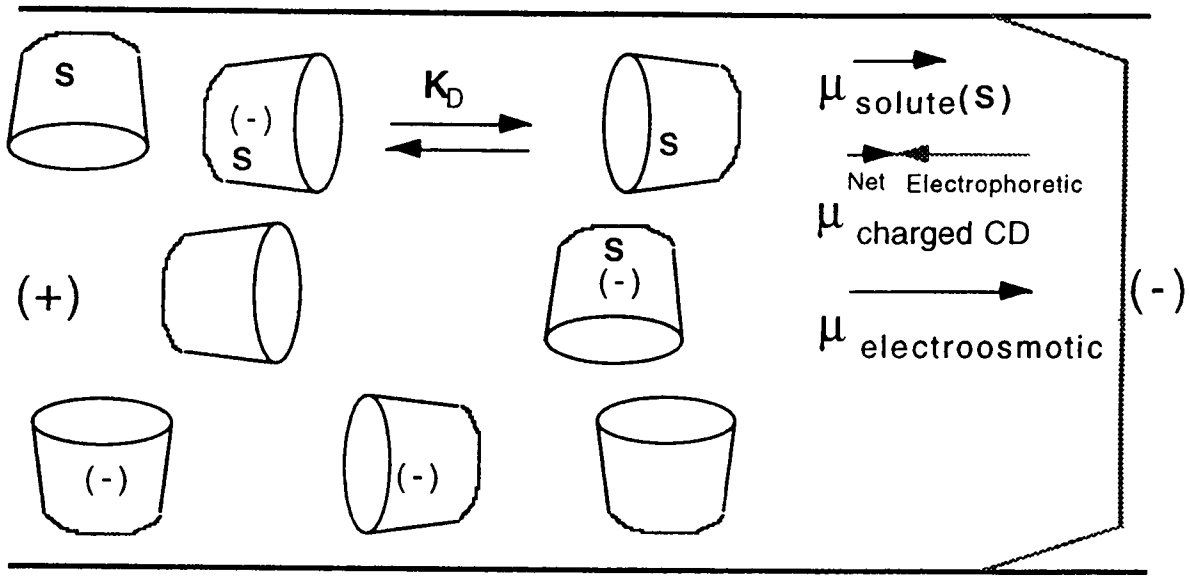

Figure 3 Depiction of flow dynamics in CDCE.

phase is more selective than the micellar phase in CD-MECC. Furthermore, many types of charged CDs (each of which can have various degrees of substitution) are readily available, leading one to believe that numerous and unique selectivities in CDCE are possible.

Chapter 3
Molecular Modeling Concepts and Applications

Concept

Prior to the creation of computers, molecular geometry was simulated using mechanical molecular models. Although these models provided some qualitative information, no quantitative conclusions could be drawn with regard to molecular structure. In many cases, the limitations in these mechanical models lead to incorrect ideas about a molecule's geometry.

Mechanical molecular models have all but been replaced by computer programs that allow one to study molecular structure. These programs fall into two main categories. The first is quantum mechanically based programs and the second uses molecular mechanics (or force fields).

The quantum mechanically based programs provide a mathematical description of molecular structure in terms of atomic nuclei and the electron distribution around them. The calculations involved in generating this type of information are time consuming and may require the use of "super computers." These two characteristics limit accurate quantum mechanical calculations to studies of small molecules (37, 38). Molecular mechanics programs have found utility over quantum mechanical programs because they can be used to study larger molecules, require much less computational time, and can be run on personal computer systems.

In the simplest sense, molecular mechanics predicts the most

energetically favorable conformations of a molecule (39). This is done by considering a molecule as a collection of points (atoms) held together by elastic forces (bonds) having different elasticities (force constants). The forces that hold the atoms together are described by potential energy functions of bond lengths, bond angles, and non-bonded interactions. The combination of these functions is the force field. The energy of a molecule in the force field is a summation of energy contributions primarily from bond stretching, bond angle bending, bending of planar atoms out of the plane, torsional energy due to twisting about bonds, and van der Waals non-bonded interactions. These parameters are calculated with respect to the "ideal" structure of the molecule in question. Therefore, molecular mechanical calculations provide an energy that is the difference between the molecule of interest and a hypothetical molecule having exactly ideal values for all of the parameters listed above. For this reason, the energy of a molecule calculated using molecular mechanics has no meaning by itself but is meaningful when comparisons between molecules are made (37-40).

Applications

Molecular mechanics has been primarily used by organic chemists to model equilibria among stereoisomers or to study the stereospecificity of reactions (41-43). It has also been used to study protein-enzyme interactions and structure-activity relationships of drug molecules (44). In relation to the molecular modeling work presented in this document (experimental details of

which are found in Chapter 4), there have been a limited number of reports, mainly by Lipkowitz et al., of comparisons of computationally derived interaction energies to chromatographic behavior (45-49).

Molecular modeling has been used to study the structural characteristics of CDs in the gaseous and solid states (50-52). Furthermore, conformational analyses of solute inclusion by CDs have been executed via molecular modeling. For example, Lu et al. performed molecular mechanical calculations on β-CD complexes and found a correlation between the van der Waals stabilization energies of the complexes and dissociation constants measured by cyclic voltammetry (53). Kostense et al., through systematic rotation and translation of the guest molecule about the central axis of the CD's cavity, were able to derive the position of the guest which results in the most favorable interaction energy with the CD (54). These authors demonstrated that their data were in good correlation with crystallographic data. Lipkowitz et al. were able to explain chiral recognition by α-CD for the enantiomers of tryptophan using molecular modeling in conjunction with ^{1}H and ^{13}C NMR studies (55).

Data obtained through molecular modeling studies have been used to describe the chromatographic behavior of solutes in HPLC (56, 57). Arnold et al. compared the retention times of several solutes using a β-CD bonded column to computationally derived interaction energies of the corresponding β-CD inclusion complexes (57). They were able to correlate interaction energies and HPLC retention times within a given series of similarly substituted

benzenes. Correlations between different classes of substituted benzene compounds were not observed.

Limitations and Considerations in Molecular Modeling Calculations

When using computer resources to solve a scientific problem, it is natural to feel confident that the data obtained are quite accurate and need not be doubted. However, this attitude is not the best one to adopt when performing molecular modeling calculations. It can generally be said that molecular modeling data are only as good as the assumptions made within the computer program used in its generation.

The biggest limitation that still exists in all molecular mechanics programs is the inability to easily reach a global energy minimum for the molecule(s) in question (40, 44). Basically, energy minimization is a series of computations in which all parameters defining the geometry of the molecule(s) are modified by small increments until an overall energy minimum is reached for the system. While the result of minimization may be the global energy minimum for the system, it is more likely to be a local minimum. To overcome the problem of local minima, it is important to minimize several different initial orientations of a molecule(s) so that different energy minima are reached.

Other limitations of molecular mechanics programs are associated with the number of atoms that can be studied at one time. Many of the PC-based programs are unable to handle molecular

systems that have a large number of atoms (58). This limitation is overcome by using a "super computer" which has the capability to study such systems. However, even though these more powerful computers can be used to study complicated molecular interactions, computational time is still a factor. Generally, the more intricate the system to be studied, the longer the analysis time.

Partially based on the limitations mentioned above, the molecular modeling studies of solute/CD interactions presented in this document (see Chapters 6-8) were designed with several common themes.

In all of the molecular modeling experiments described in the chapters that follow, attempts were made to study all proper and logical orientations between solute and CD molecules (see Chapter 4 for procedure employed). This is necessary because, as discussed above, problems of getting "stuck" in local minima exist in most modeling programs, including the SYBYL molecular modeling program used in this work. Therefore, by sampling many possible solute/CD orientations, one can be assured that one of the local minima calculated is actually the global minima and thus the best interaction energy between the molecules in question. One drawback of sampling many possible orientations is that of time. If one were to sample all possible orientations between several sets of molecules, a graduate degree would require innumerable years to complete. As this was not the goal of this author, modeling studies were designed to sample only the most logical orientations. Furthermore, as is discussed below and in subsequent chapters, the

global minimum interaction energy is not necessarily the most important piece of information when comparing molecular modeling data to separation behavior.

In some cases it is important to allow relaxation of the solute and CD molecules at each position by employing the MINIMIZATION function of SYBYL. This routine allows the atoms and bonds within each molecule of the complex to rearrange, without changing the centers of mass of the molecules, in the calculation of an interaction energy. However, minimization is computationally intensive, therefore time consuming, so its application in the modeling studies described in this document was limited. In our experience, the use of the minimization routine was most important in describing separations of enantiomers that contain a chiral atom (i.e. DNS-amino acids). Separations of such compounds, via complexation with CDs, are based on very specific interactions that differ only slightly in energy between each enantiomer and a CD molecule. In order to highlight this small difference in interaction energies, minimization of each enantiomer/CD complex was necessary.

Once collected, interaction energy data must be properly interpreted. While some information can be gleaned from determination of global interaction energy minima, other methods of data treatment have proven more accurate in explaining separation behavior. Since CE separations employing CD additives are dynamic in nature, it can be expected that the solute molecule in some of the transient, solute/CD complexes is not in a global energy minimum

position. However, these "non-optimum" complexes are still energetically favorable enough to exist. For this reason, an average or summation of various portions of the energy information from studying many conformations leads to a more complete description of CE separation behavior.

Finally, it is sometimes appropriate to consider such parameters as solvation, entropy, and energy barriers when calculating interaction energies. Solvation can be simulated using the SYBYL molecular modeling software, but such studies substantially add to the already lengthy calculation processes. Furthermore, its effects, as well as those of entropy and energy barriers on the interaction energy calculations performed by these authors were assumed to be similar, and therefore could be ignored, as the compounds in each study were structurally similar.

Chapter 4
Experimental

Capillary Electrophoretic Studies

apparatus

separation

The typical CE experimental apparatus is depicted in Figure 4. Basically, it consisted of a measured length of fused silica capillary (specific lengths and i.d.s specified where appropriate) purchased from Polymicro Technologies, Inc. (Phoenix, AZ, USA). The capillary was suspended between two microcentrifuge vial buffer reservoirs that were adjusted to equal heights to eliminate hydrostatic flow. The separation voltage was supplied via platinum electrodes placed in the reservoirs using a Hipotronics (Brewster, NY, USA) model 840A high-voltage power supply. Data were collected by a Kipp and Zonen (Delft, Holland) model BD40 strip chart recorder.

detection

Depending upon the characteristics of the solutes of interest, one of two different detection schemes was employed. When absorbance detection was appropriate, a Linear (Reno, NV, USA) model 204 ultraviolet-visible detector with a CE flow cell adaptor was employed. Detection wavelengths are specified where appropriate.

In instances where the advantages of laser-based fluorescence detection could be exploited, excitation was provided by an

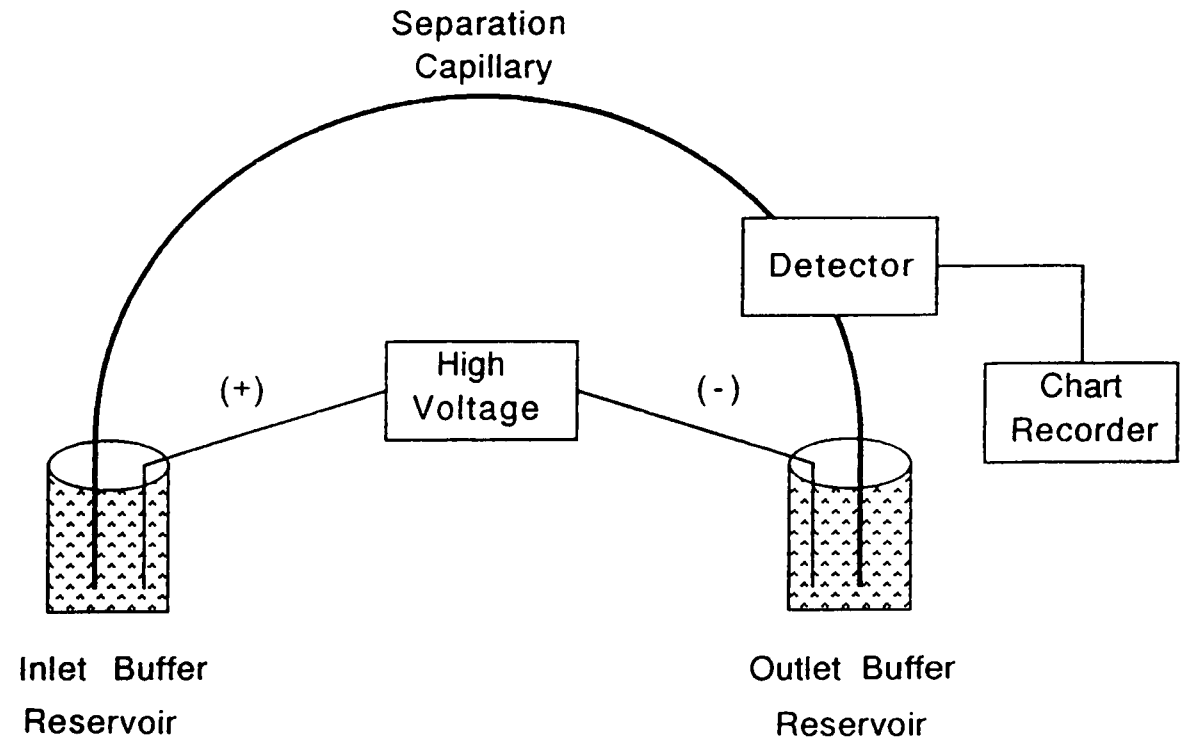

Figure 4 General depiction of CE apparatus.

Omnichrome (Chino, CA, USA) model 3074-20M He-Cd laser (20 mW, 325 nm). The laser beam first passed through a 325 nm laser line filter. The beam was then focused through the capillary, which was affixed to an aluminum cell holder and mounted in a fiber optic positioner (Newport Research Corp., Irvine, CA, USA), using an f/1 biconvex quartz lens. One of two means of collecting fluorescence emission was employed. In some cases (see Figure 5), the emission was collected and collimated using an f/1 biconvex glass lens and passed through a didymium filter (cut on at 360 nm; average % transmittance of 50% from 370 to 570 nm) for wavelength isolation. The emission was then focused, using an f/2 biconvex glass lens, through a 0.5 mm slit which was contained in a light-tight box that was fitted to the photomultiplier tube (PMT) housing. The emission was detected with a Hammamatsu (Bridgewater, NJ, USA) model R212 PMT. A Pacific Photonics (Concord, CA, USA) model 126 photometer served as both PMT power supply and signal processing electronics.

In other instances (see Figure 5), the fluorescence emission was collected using a 600 μm (core) diameter fiber optic positioned adjacent to the detection region of the capillary. The opposite end of the fiber optic was flush with a didymium filter (see above) which preceded the entrance to a Hamamatsu (Bridgewater, NJ, USA) model HC120-01 PMT, which was powered by an in-house constructed supply. The detector output was directed through a noise filter and signal offset circuit that consisted of a selectable RC time constant and a difference amplifier for removal of any

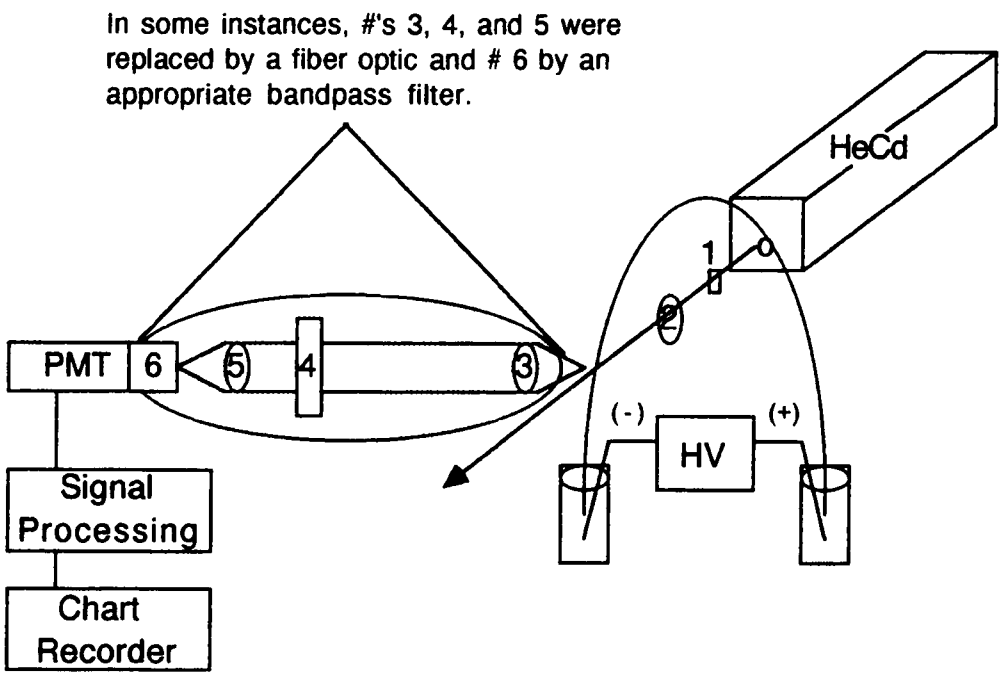

Figure 5 Depiction of laser-based fluorescence detection schemes. Optical components: 1) 325 nm laser line filter, 2) f/1 biconvex quartz lens, 3) f/1 biconvex glass lens, 4) didymium filter, 5) f/2 biconvex glass lens, and 6) light-tight box containing 0.5 mm slit.

constant background signal and was also built in-house (see reference 59 for detailed information regarding the construction and use of these in-house built items).

chemicals

separation buffer components

All solvents were HPLC grade and were purchased from Baxter Scientific Co. (McGaw, IL, USA). Buffer (NaH_2PO_4 and $Na_2B_4O_7$) and surfactant [SDS and sodium cholate (NaC)] reagents were purchased from Sigma Chemical Co. (St. Louis, MO, USA) or from Aldrich Chemical Co. (Milwaukee, WI, USA) and were reagent grade or better. Native CDs (α and β) were purchased from Sigma Chemical Co. (St. Louis, MO, USA), while native γ-CD was purchased from Pharmatec, Inc. (Alachua, FL, USA). All derivatized CDs (carboxymethyl (CM)β, hydroxypropyl (HP)β, and HPγ) were gifts from American Maize Products (Hammond, IN, USA) or CTD, Inc. (Gainesville, FL, USA).

sample components

PAH samples were obtained from Aldrich Chemical Co. (Milwaukee, WI) or donated by the National Cancer Institute Chemical Carcinogen Repository (Kansas City, MO). 5-Dimethylamino-1-naphthalene sulfonyl (DNS)-amino acids; including leucine (Leu), valine (Val), threonine (Thr), serine (Ser), glutamic acid (Glu), and aspartic acid (Asp) were purchased from Sigma Chemical Co. (St. Louis, MO, USA). 1,1'-Bi-2-naphthol [$BN(OH)_2$] and 1,1'-binaphthyl diyl hydrogen phosphate ($BNPO_4$) were purchased from Aldrich Chemical Co. (Milwaukee, WI, USA), while 1,1'-

Binaphthyldicarboxylic acid [$BN(COOH)_2$] was supplied by Dr. W. L. Hinze, Wake Forest University (24).

procedures

Separation buffers were prepared by dissolving the appropriate amount and type of surfactant, CD, or combinations of the two, in a buffer which was composed of 10 mM NaH_2PO_4 and 6 mM $Na_2B_4O_7$. Typically, this buffer was prepared and used at pH 9. However, in some cases, the pH was raised or lowered using concentrated NaOH or H_3PO_4, respectively. When organic solvents were employed as modifiers, they were incorporated in the separation buffer and are reported in terms of percent volume/volume (% v/v).

All stock solutions were 1 mM in solute concentration. Those of PAHs and BNs were prepared by adding the appropriate type and mass of solid to tetrahydrofuran (THF) and sonicating for 30 min to ensure complete dissolution. Stock solutions of the DNS-amino acids were prepared as above except the solvent was the separation buffer to be used in the separation.

Sample solutions to be injected were prepared by diluting appropriate volumes of the stock solutions with the separation buffer to be employed. Typically, these solutions were $1X10^{-2}$ mM in concentration when absorbance or $1X10^{-4}$ mM in concentration when laser-based fluorescence detection systems were employed.

Capillaries were prepared by cutting a desired length and removing part of the polyimide coating with a flame to create a detection region. A syringe needle was affixed to the inlet end to

facilitate rinsing. If laser-based detection was to be employed, the capillary was mounted in a cell holder at the point of detection. Capillaries were rinsed with 100 mM NaOH for 10 min followed by a separation buffer rinse for an additional 5 min. The operating voltage was applied for 10 min prior to the first sample injection.

Samples were injected either hydrostatically or by electromigration. Hydrostatic injections were performed by placing the inlet end of the capillary into the sample solution and raising it 10 cm above the outlet end for 10 sec. The capillary was then returned to the inlet reservoir and the operating voltage was applied. Injection by electromigration was accomplished by replacing the inlet reservoir with the sample vial and applying a voltage of 2 kV for 30 sec. The inlet reservoir was then returned to its original position and the operating voltage was applied. Typical injection volumes were 0.5 to 1 nL and 2 to 4 nL, for 25 μm and 50 μm i.d. capillaries, respectively.

Duplicate injections of each sample were performed manually. Peak identification was accomplished by sequential addition of individual solutes to the sample solution or by "spiking" the sample with the solute of interest. Column void time (t_o) was marked by a baseline solvent disturbance resulting from trace amounts of solvent present in the sample solution or from the addition of acetone (0.01% v/v) to the sample solution. The migration time of the micellar (t_m) and charged CD (t_{ch}) phases were marked by the migration times of benzo(a)pyrene (BaP) and anthracene, respectively, as these compounds associate very strongly with

these phases.

data manipulation

Plots appearing herein were generated using an IBM-clone computer (Gateway 2000); 33 MHz 80386DX with 80387 co-processor, 8 MB RAM, employing the TableCurve 3.0 plotting program developed by Jandel Scientific (San Rafael, CA, USA). This program contains over 200 stored equations that are sampled and those that best fit the data supplied are used to generate plots. The program also calculates values for the constants contained in the fitted equations.

safety

Benzopyrene compounds are known carcinogens and the other PAHs are suspected carcinogens, so extra caution was exercised when working with these compounds. All PAH solutions were prepared under a ventilated hood and disposable latex gloves were worn while working with these compounds. Care was taken to dispose of all waste solutions properly.

Molecular Modeling Studies

apparatus

Solute/CD interaction energies were calculated using the SYBYL 6.0 molecular modeling software developed by Tripos Associates, Inc. (St. Louis, MO) and run on an Evans & Sutherland

ESV-3 workstation (Salt Lake City, UT). This UNIX-based, high-performance, 3D graphics workstation's CPU is implemented with a 25 MHz MIPS R3000 RISC microprocessor. There is a total of 128 Kbyte of high-speed cache memory and the system memory ranges from 8 up to 129 Mbytes (60). Structures of all solutes were constructed using the SKETCH routine of the software. When constructing the enantiomeric pairs of the DNS-amino acid and BN compounds, one enantiomer was created and the INVERT function was used to generate the other enantiomeric form. α, β and γ-CD structures were generated using crystallographic coordinates imported from the Cambridge Crystallographic Database (Cambridge, England). Prior to use, Gasteiger-Huckel charges, which are a summation of the σ and π components of the atomic charge, were assigned to all structures which were then minimized using the MINIMIZATION function of SYBYL. A convergence limit of 0.05 kcal/mol and a maximum number of iterations of 100,000 were designated to ensure complete minimization.

A reference point, typically the center of mass, was defined for each molecule prior to use. This point, termed a centroid, was necessary for the initial positioning and all subsequent movements, of the solute and CD molecules in the generation of interaction energy matrices. Centroids were defined for the benzopyrene and CD molecules as the point marking the center of mass of the molecule. The DNS-amino acid anion centroids were defined as the point marking the center of the naphthalene group in the DNS. The centers of the BN enantiomers were defined as the center of the naphthalene

ring to be included into the CD.

procedures

The SYBYL Programming Language (SPL) was used to generate a routine that permitted operator control over solute/CD positioning prior to energy calculations. Specifically, the SPL routine allowed the solute's position to be systematically altered relative to the CD cavity (see Figure 6 for perspective on positioning). The initial and final positions of the solute relative to the CD (as defined by the distance between the centroids of the molecules), translational increments, and rotational increments could all be specified within the routine. The total energy of the complex was computed and recorded at each translational/rotational position. The specific values of starting positions and increments employed were dependent upon the molecules studied and are presented in conjunction with experimental results.

The interaction energy of the complex at each of these positions was calculated by subtracting the energies of the uncomplexed solute and CD molecules from the total energy values obtained. Thus, a three-dimensional energy matrix (translation/ rotation/energy value) was generated. A plot of one such energy matrix appears in Figure 7. In some instances, the MINIMIZATION function of SYBYL was employed starting at selected of these positions, with the maximum number of iterations defined as 100,000 to ensure complete minimization.

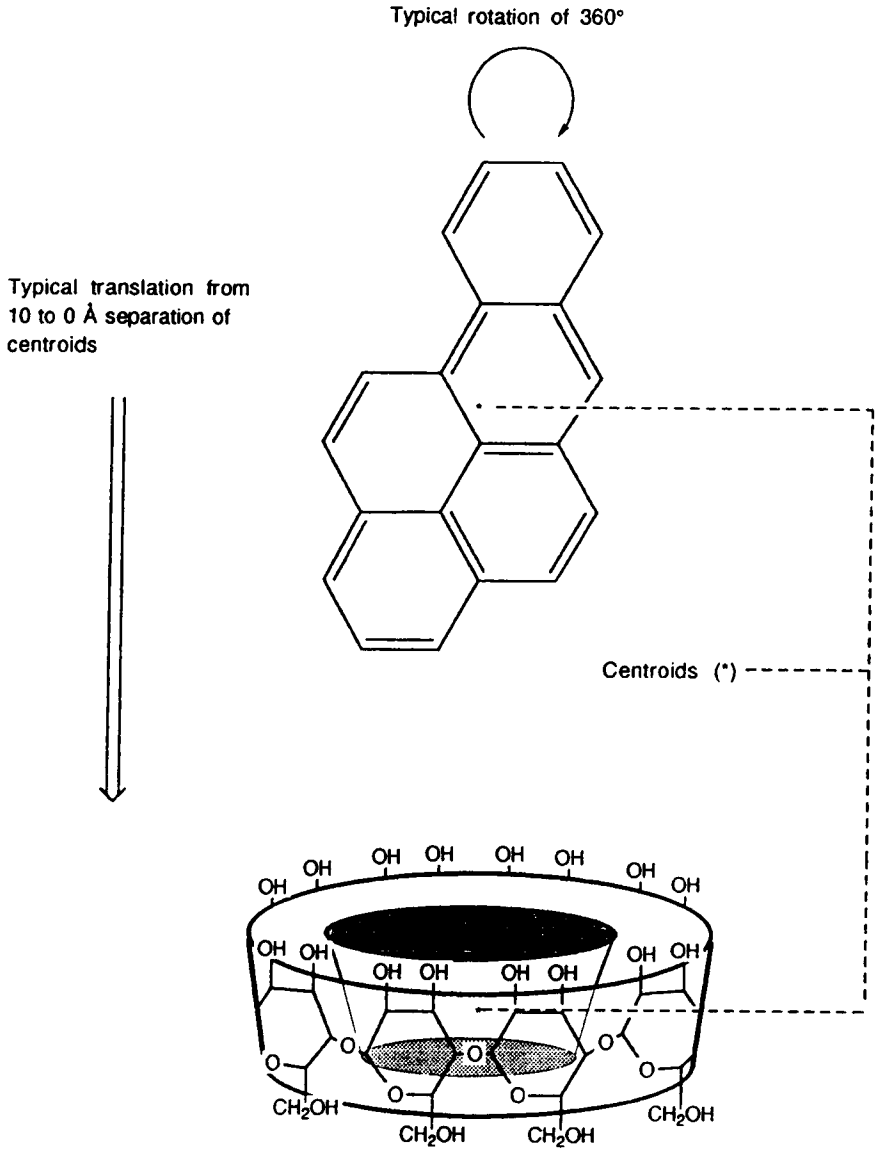

Figure 6 Depiction of molecular positioning and movement in molecular modeling studies.

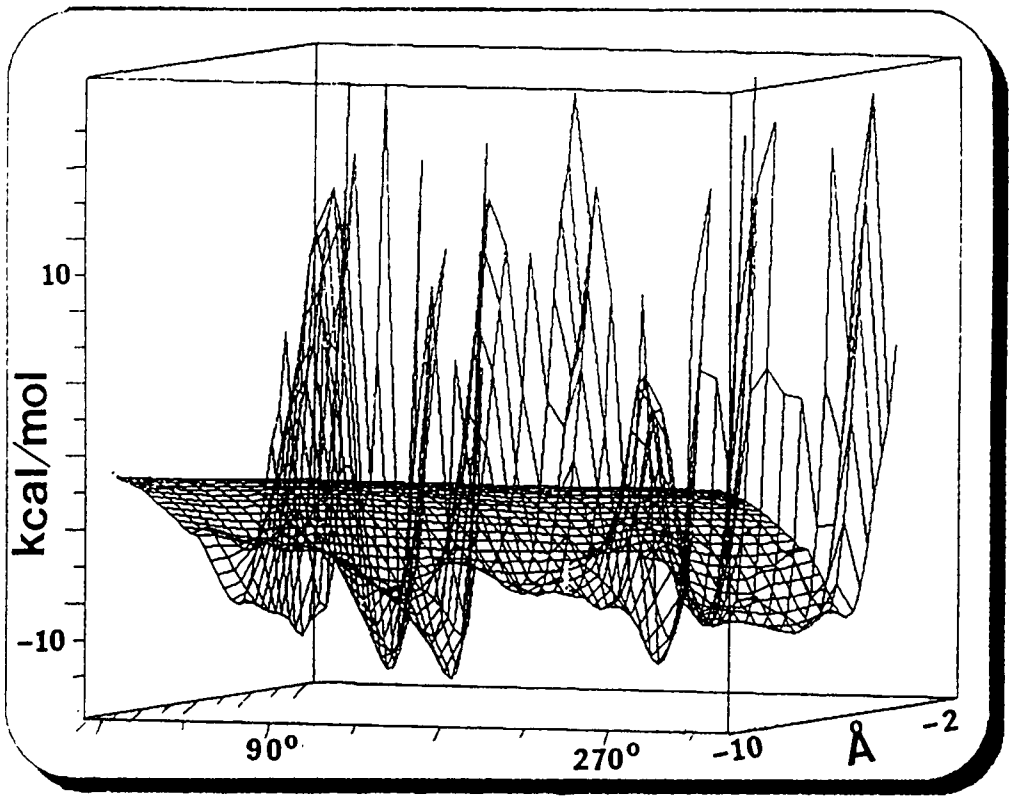

Figure 7 Three-dimensional plot of typical molecular modeling results.

In selected cases, the SYBYL DOCKING routine was used to locate interaction energy minima starting at given translational/rotational positions. However, this was very time consuming and generally not employed. In other situations, some of the most energetically favorable solute/CD complexes were constructed and solvated prior to minimization. In a portion of the BN work, the DISPLAY H-BONDS function of SYBYL was used to identify hydrogen bonds in some minimized complexes.

The data collected in the matrices was treated in different manners to determine an inclusive interaction energy that served to represent the strength of the dynamic interaction between solute and CD. One method of data treatment included averaging the interaction energies of the five most energetically favorable positions. Another method of data treatment involved representing the inclusive interaction energy as a simple statistical mechanical partition function (Z) calculated by summing over all the values in the matrix using the equation:

$$Z = \Sigma\, e^{-E / kT} \qquad [8]$$

where E is the interaction energy, k is the Boltzmann constant, and T is defined as 298 K.

Chapter 5
Cyclodextrin-Modified Micellar Electrokinetic Capillary Chromatographic Separations of Polycyclic Aromatic Hydrocarbons

Introduction

PAHs are formed by thermal decomposition of any organic material containing carbon and hydrogen. Specific methods by which they are formed include pyrolysis, incomplete combustion, or carbonization processes. Since PAHs are the largest single class of chemical carcinogens, much energy has been expended to develop methods to isolate and analyze these compounds (61).

GC techniques have been used extensively in the analysis of PAHs but are continually hindered by the low volatility and thermal instability of these compounds (62). HPLC is another viable method for PAH isolation from complex mixtures (63). However, this technique also has its limitations. Mainly, the low efficiency and peak capacities attainable in HPLC result in inadequate separation of PAHs. Capillary LC has also been employed for the separation of PAHs (64, 65). Fundamentally, this technique solves the volatility problems associated with GC and the efficiency and peak capacity limitations present in HPLC. However, capillary LC has its own pitfalls. Packed capillaries lead to long analysis times, and the small diameters of open capillaries give rise to problems associated with bonding stationary phases to their walls (66, 67).

MECC has proven to be a successful alternative to the separation techniques mentioned above. MECC exhibits very high efficiencies (plate numbers up to 10^5 or 10^6 plates/m) and employs mobile phase additives rather than bonded phases. As a result of the small capillary i.d.s utilized in MECC (typically 25 or 50 μm), only minimal volumes of samples and mobile phases are required. These small volume requirements lead to advantages in PAH separations including the ability to use expensive mobile phase additives (including CDs) and the production of limited amounts of hazardous PAH waste. Furthermore, MECC mobile phases can be quickly and easily replaced as compared to those of other separation methods (20).

Also advantageous to MECC separations of PAHs is the ability to employ one of two detection methods. Absorbance detection is easily compatible with PAH separations as their aromatic character results in strong absorbance bands at 254 nm (63). However, the more sensitive method of fluorescence detection can also be utilized. The PAHs exhibit relatively strong fluorescence, which can be enhanced by the hydrophobic environment of the micelles and/or CDs (68). Limits of detection in such a system, based on injected quantity, for anthracene, pyrene, and BaP have been reported as 9×10^{-7}, 4×10^{-7}, and 2×10^{-7} M, respectively (21).

Results and Discussion

system retention

Even with the high efficiency and versatility of MECC, resolution of highly hydrophobic compounds, such as PAHs, is often difficult. Careful optimization of mobile phase conditions, including organic modifier and micelle types and concentrations, is necessary in most cases.

Resolution partially depends upon the breadth of the elution range (t_o/t_m) (see Equation [6] in Chapter 2). Alcohols, such as 2-propanol and methanol (MeOH), can be added to the MECC mobile phase to extend the elution range (18). This extension is a result of the change in the zeta potential at the capillary wall, due to the interactions of these alcohols with the silanol groups, leading to a reduction in electroosmotic flow. However, the increase in resolution as t_o/t_m approaches zero (indicating an infinite elution range) is offset by the resulting increase in analysis time. Acetonitrile (ACN), while extending the elution range much less than alcohols, can also be used as an organic modifier in MECC. It acts to reduce k' values by providing a more hydrophobic bulk mobile phase which alters the partition coefficient of solutes between bulk and micellar phases (see Chapter 2). The elution range and solute retention time can be used to calculate a capacity factor (k') (see Equation [7] in Chapter 2). Proper adjustment of elution range will lead to optimum k' values which fall between 1 and 5 (31). However, the highly hydrophobic PAHs tend to completely associate with an

SDS micellar phase and co-elute at t_m (solutes with k' values > 25 tend to be unresolved in MECC). By employing organic modifiers in an SDS micellar system, the k' values of some PAHs can be decreased but only to a small extent (see above). One means of reconciling this problem is using naturally occuring bile salt surfactants in place of SDS. The bile salt micelles are reported to be less hydrophobic than SDS micelles and more resilient to organic solvents (69). MECC separations employing bile salts, such as NaC, can therefore be expected to result in reduced k' values as compared to those using SDS.

The data presented in Table I demonstrate the effects of organic modifier type and concentration and NaC concentration on separations of four PAHs. The reductions in PAH k' values with increasing ACN concentration are dramatic. Three of the test compounds exhibit optimum k' values at the highest (30%) ACN concentration. Naphthalene, being the least hydrophobic of the test solutes, exhibits an optimum k' with 10% ACN present. Increasing the bile salt concentration from 50 to 100 mM results in an undesirable increase in k'. This is due to the dependence of capacity factor on the thermodynamic partition coefficient (K) and phase ratio (β) as seen in the expression:

$$k' = K\beta \qquad [9]$$

where β is given by the ratio of micellar volume to mobile phase volume, and increases with increasing surfactant concentration.

Table I. MECC k' values of several PAHs.

	50 mM NaC				100 mM NaC	
	0 % ACN	10% ACN	20% ACN	30% ACN	30% ACN	30% 2-prop
PAH (k')						
naphthalene	6.30	1.88	0.921	0.531	2.98	4.90
anthracene	46.6	17.3	5.99	1.57	17.4	9.00
pyrene	85.4	46.2	14.7	3.18	40.7	15.8
chrysene	t_m	107	40.8	6.09	112	67.1
t_o	5.86 min	6.83 min	7.22 min	9.56 min	9.62 min	12.5 min
t_m (BaP)	13.7 min	16.1 min	16.3 min	16.2 min	30.0 min	36.2 min

The extension of the elution range by organic modifier addition is evident in the values of t_o and t_m in Table I. The 2-propanol slows electroosmotic flow to a much greater extent than ACN as seen by the larger t_o value for the 2-propanol system. Even though the t_o and t_m values in Table I demonstrate a broader elution range in the 2-propanol system verses the ACN systems, this difference should be greater, but the value for t_m is no longer valid at such high organic modifier concentrations. At such concentrations, the solute used to mark t_m, BaP in this case, is no longer completely associated with the micelle and thus does not have a k' of infinity.

selectivity

Depending on the physiochemical properties of the components to be separated, changes in MECC operating conditions such as organic solvent addition or micelle concentration alteration can influence selectivity but will not always lead to adequate resolution (70). In these cases, resolution can be increased by the greater selectivity resulting from addition of CDs to the MECC mobile phase (71).

In CD-MECC separations of PAHs, the micelles serve two purposes. First, they function to increase the solubility of these compounds in the aqueous mobile phase. Secondly, but more importantly, they impart a mobility to the PAHs (which are neutral and otherwise would co-elute at t_o) thus causing them to elute at or near t_m. The neutral CDs employed in this work have no intrinsic mobility and thus move at the electroosmotic velocity. Therefore,

solutes partitioning between the CD and micellar phases will exhibit retention times that fall somewhere between t_o and t_m and have values of k' between zero and infinity. The magnitude of k' is partially a result of the strength of the inclusion complex formed between the solute and CD, which is determined by the size, geometry, and physiochemical properties of each (21, 71).

The electropherograms presented in Figure 8 demonstrate the selectivity provided by several types of CDs in the CD-MECC separation of several three, four, and five-ring PAH isomers. Specifically, SDS micelles and either HPβ or γ-CD or native γ-CD were employed. SDS, rather than NaC, was the surfactant of choice because of its compatibility with CDs. The steroidal structure of NaC allows for the formation of inclusion complexes between it and the CD thus inhibiting inclusion complex formation between CD and solute molecules (72).

In Figure 8A, discrimination between substitutional isomers by CDs is demonstrated using anthracene, two of its methyl (Me) derivatives, and BaP as solutes. It was necessary to include 10% ACN in the mobile phase to optimize the k' values of these compounds. But complete resolution was only obtained when the moderately sized HPβ-CD was added to the SDS mobile phase.

Figures 8B and C show the separation of several four-ring isomers, including pyrene, chrysene, benz(a)anthracene and BaP. In B, the largest derivatized CD used in these studies, HPγ-CD, in conjunction with 20% ACN, provided near-baseline resolution of these compounds. The polydispersity and high degree of substitution

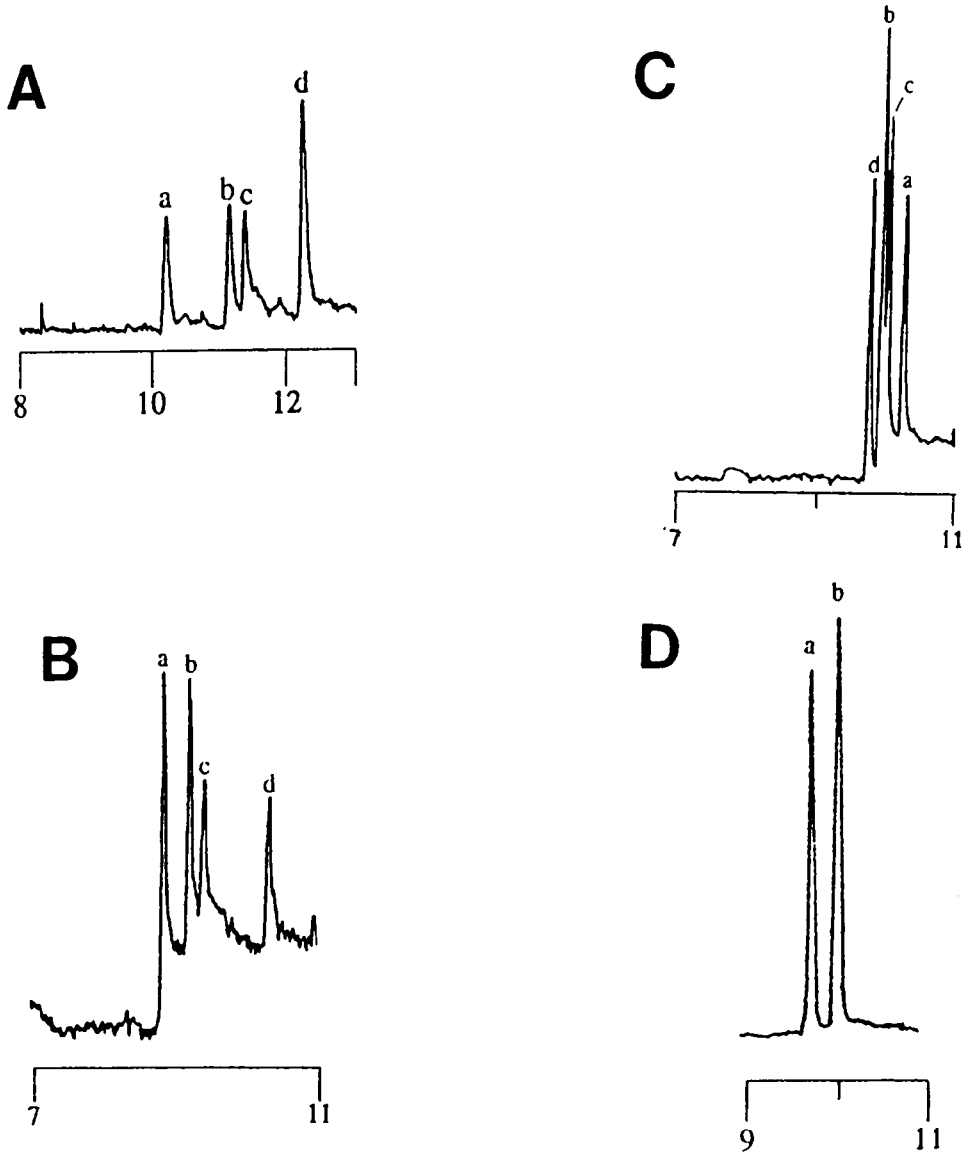

Figure 8 CD-MECC separations of PAHs. Solutes and conditions: **A)** anthracene (a), 2-Me anthracene (b), 9-Me anthracene (c), and BaP (d) using 25 mM HPβ-CD and 10 % ACN. **B)** pyrene (a), chrysene (b), benz(a)anthracene (c), and BaP (d) using 25 mM HPγ-CD and 20 % ACN. **C)** same solutes as B) using 10 mM γ-CD. **D)** BaP (a) and BeP (b) using 10 mM γ-CD. Note: all mobile phases contained 50 mM SDS.

(~7 HP groups/CD) of the HPγ-CD sample does not provide adequate discrimination between the subtle geometric differences of these four-ring PAH isomers. Therefore, addition of ACN to the HPγ-CD mobile phase was necessary to lead to the resolution observed. Interestingly, the elution order was significantly altered when γ-CD was employed (see Figure 8C). The increased selectivity provided by γ-CD is a result of its unhindered cavity and sample uniformity (as compared to HPγ-CD) which lead to better inclusion of the four-ring isomers. γ-CD forms an especially strong inclusion complex with BaP (as evidenced by its eluting prior to all of the four-ring isomers). For this same reason, it was possible to resolve BaP from another five-ring PAH, benzo(e)pyrene (BeP) using γ-CD (see Figure 8D).

Chapter 6
Cyclodextrin-Modified Micellar Electrokinetic Capillary Chromatographic Separations of Benzopyrene Isomers: Correlation with Computationally Derived Interaction Energies

Introduction

Native CDs have been shown to improve CE/MECC separations by imparting unique selectivity based on solute size and geometry or through chiral recognition (21, 26, 73-75). Derivatized CDs, such as the HPγ derivative used in this work, have also been used as mobile phase additives (21, 26). While these reports demonstrate the utility of CD mobile phase additives, they provide little fundamental information regarding the chromatographic characteristics of CD separation systems. In particular, the interaction energies between the CD and the solute have not been correlated with separation performance. Such correlations could provide useful guidelines for designing capillary electrokinetic separations involving various CDs (see below), or other organized media.

The work reported in this chapter concerns the chromatographic behavior of benzopyrene isomers in CD-MECC. Benzopyrene compounds are members of an important class of compounds, the PAHs. PAHs are a significant type of environmental pollutant. One particular benzopyrene isomer, BaP, has been shown to be carcinogenic (61). This creates a need to develop analytical methodologies for isolating and characterizing benzopyrenes. In

previous work, we noticed a very strong interaction with γ-CD (see Chapter 5). The magnitude of this interaction provided impetus for the studies presented in this chapter.

Computer-aided molecular modeling and conformational analyses of solute inclusion by CDs have been performed by other researchers, and some of these studies, which are significant to this work, have been summarized (see Chapter 3). Similar studies could be useful in explaining the effects of CD additives in MECC.

In this chapter, effective separations of various benzopyrene isomers are demonstrated, and the effects of CDs and other mobile phase components on retention are illustrated. Efforts to correlate the retention behavior of benzopyrene isomers in CD-MECC with computationally derived solute/CD interaction energies are also described. Such correlations are complicated by the complex and dynamic nature of CD-MECC. In this separation system, CD and mobile phases are transported at the electoosmotic flow velocity, which is very dependent on experimental conditions (20). The micellar phase is electrophoretically retarded and involves a dynamic equilibrium between free surfactant and micelle. Moreover, solute/micelle association can occur by a variety of mechanisms, and solute/CD interactions do not necessarily require inclusion complex formation (20, 57). The general effect of solute/CD interaction is to reduce retention times by inhibiting solute/micelle association. Despite the aforementioned complications, elution order for most of the benzopyrene isomers studied are correctly predicted based on calculations of solute/CD interaction energies.

Results and Discussion

general separation considerations

One approach to the separation of hydrophobic compounds involves adding CD to the MECC mobile phase. In addition to specific solute/CD interactions, the CD can function in a general sense to impart organic character to the mobile phase and thereby reduce k'. The distribution of BaP between aqueous (aq), CD, and micellar (M) phases can be expressed in terms of the micellar-aqueous (K_M), CD-aqueous (K_{CD}), and CD-micellar (K_{CD-M}) distribution coefficients as depicted below.

$$BaP_{(aq)} \text{ <--> } BaP_{(Micelle)}$$

$$K_M \quad \uparrow \quad \vdots \quad \downarrow$$

$$K_{CD-M} = [BaP]_{CD}/[BaP]_M \qquad (10)$$

$$BaP_{(aq)} \text{ <--> } BaP_{(CD)}$$

$$K_{CD}$$

The exchange of benzopyrene isomers between CD and micellar phases can occur in a stepwise fashion involving the processes labeled K_M and K_{CD} (in which case $K_{CD-M} = K_{CD}/K_M$). Alternately, direct exchange of isomer between electroosmotically migrating CD and electrophoretically retarded micelle can occur. For reasons discussed below, we feel the latter mechanism is operative in these

studies. In either case, the value of K_{CD-M} should be directly related to the stability of a CD/isomer complex and the relationship between the K_{CD-M} values of the isomers should determine elution order.

The addition of 20 mM SDS produces a chromatographic phase ratio (micellar volume/mobile phase volume) that can be calculated as described by Terabe, et al. (31). Using 0.87 mL/g as the partial specific volume and 8 mM as the cmc of SDS, the phase ratio is 2.5 x 10^{-3}. Similarly, employing a reported cavity volume of 472 Å, the CD to mobile phase volume ratio is 2.9 x 10^{-3} for 10 mM γ-CD (35). Thus, the volumes of the CD and micellar phases are roughly equal and an observed k' value of unity would indicate K_{CD-M} is approximately one.

The phase ratio calculation assumes that the CD does not effect the micellization process. Using a dye solubilization procedure to measure cmc (69), we noted only a modest increase in the cmc values of both NaC and SDS in the presence of γ-CD. However, the steroidal structure of NaC is reported to facilitate the formation of stable CD inclusion complexes (76). This is supported by our separation experiments that indicate that CD and NaC are not compatible. For example, Figure 9 demonstrates the effects of γ-CD on the MECC separation of BaP and BeP using SDS and NaC micellar systems. The addition of γ-CD to the SDS system results in a general and selective reduction in k' and baseline resolution of the isomers, while the NaC system shows no noticeable effect upon addition of CD.

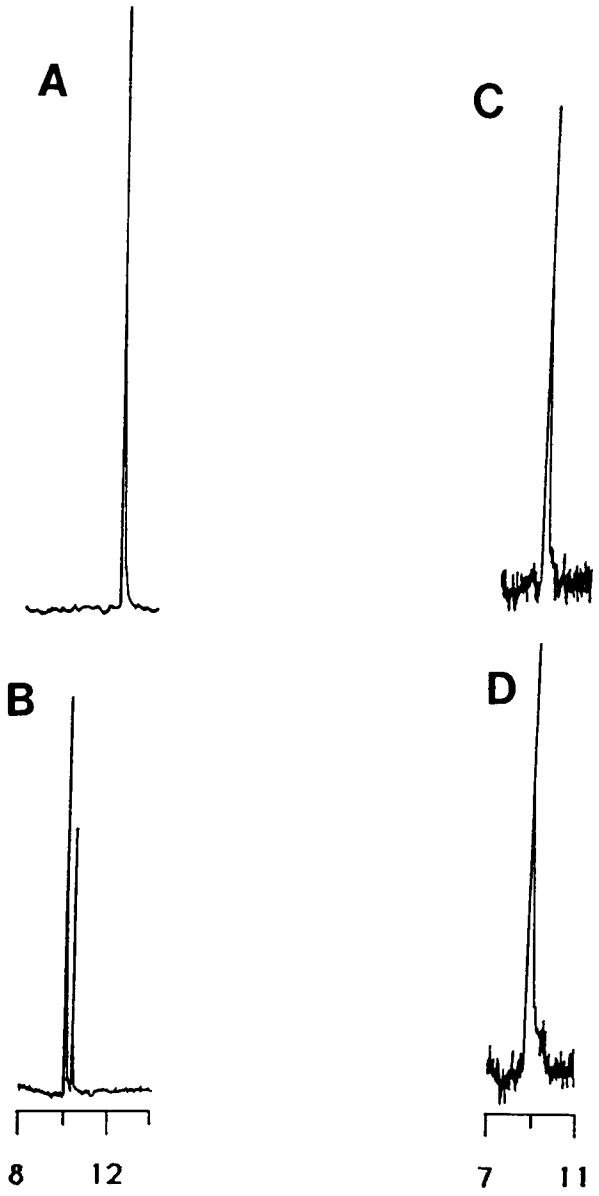

Figure 9 Comparison of SDS and NaC mobile phases for separation of BaP and BeP. Conditions: **A)** 50 mM SDS, **B)** 50 mM SDS and 10 mM γ-CD (BaP eluting first), **C)** 50 mM NaC, D) 50 mM NaC and 10 mM γ-CD.

Table II and Figures 10 and 11 illustrate the retention characteristics of MECC using SDS/CD mobile phases for separations of benzopyrene isomers. Approximate k' values found in Table II were calculated as described by Terabe, et al. using Equation (7) in Chapter 2 (31). Typically, a hydrophobic molecule that associates completely with the micelle can be used to measure t_m. However, when using mobile phases that contain γ-CD, we have yet to find a compound for which retention time (t_r) is not altered by the presence of the CD; e.g., the PAH coronene (MW 300) exhibited almost as strong of an interaction with γ-CD as BaP, despite being much larger than the γ-CD cavity dimension. For this reason, t_m was measured by injecting BaP into a mobile phase system containing no CD (i.e., $t_m = t_r$BaP without CD). Subsequently, duplicate injections of the separation mixture (containing various combinations of benzopyrene isomers) were performed using a mobile phase containing CD, followed by another measurement of t_m. The values of t_m, t_o, and t_r used to calculate k' are averages from these injections.

The k' data for the first two columns of the table was obtained by using 50 μm i.d. capillaries and UV absorbance detection, while the γ-CD data in the table and the chromatograms were generated with 25 μm i.d. capillaries and laser fluorometric detection. BaP has an infinite k' and co-elutes with the other isomers when CD is not included in the mobile phase. For comparative purposes, the last column of the table provides k' data for a straight SDS mobile phase system that includes a large concentration of acetonitrile (22.5%)

Table II. CD-MECC k' values of several BaP isomers.

Solute [10^{-5} M]	β-CD[a]	HPγ-CD	γ-CD[b] run 1	γ-CD[b] run2	no CD[c]
BaP	41	3.5	1.4	1.5	14
1-Me BaP	35	4.2	20	20	>50
3-Me BaP	30	3.8	2.1	2.2	42
5-Me BaP	30	4.2	4.8	5.0	38
6-Me BaP	21	3.7	29	29	23
7-Me BaP	26	4.2	18	18	30
10-Me BaP	23	6.4	22	22	25
1,6-diMe BaP	23	5.2	- -	- -	>50
7,10-diMe BaP	19	5.4	- -	- -	>50
BeP	- -	- -	1.7	- -	9.3
1-hyd BaP	- -	- -	1.8	- -	- -
1-eth BaP	- -	- -	17	- -	- -

a) mobile phase contains 20 mM SDS and 10 mM CD.
b) mobile phase contains 20 mM SDS, 15 mM CD, and 5% 2-propanol.
c) mobile phase contains 20 mM SDS, 22.5% ACN, and 5% 2-propanol.

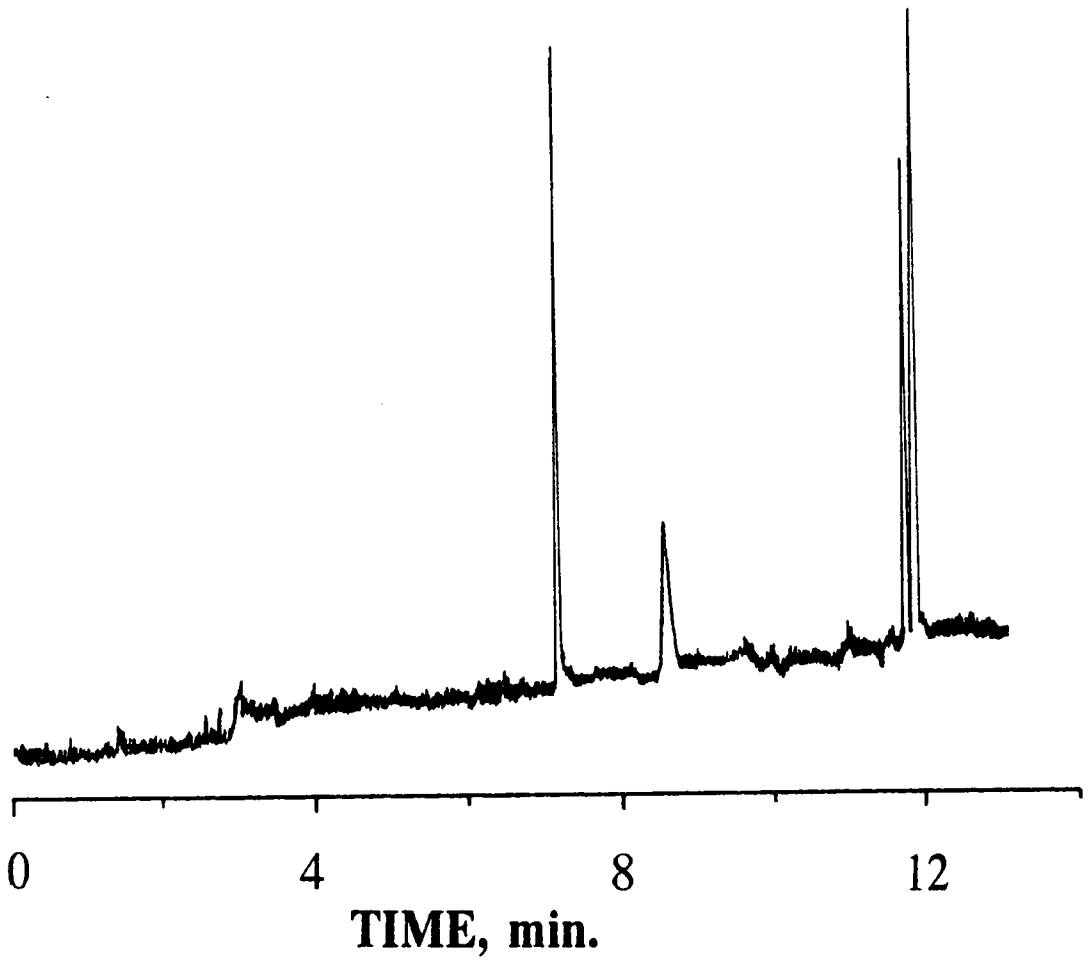

Figure 10 Separation of 1-position-substituted BaP isomers. Solutes (in elution order) and conditions: BaP, 1-hyd BaP, 1 eth-BaP, 1-Me BaP; 20 mM SDS and 10 mM γ-CD with 5 % 2-propanol.

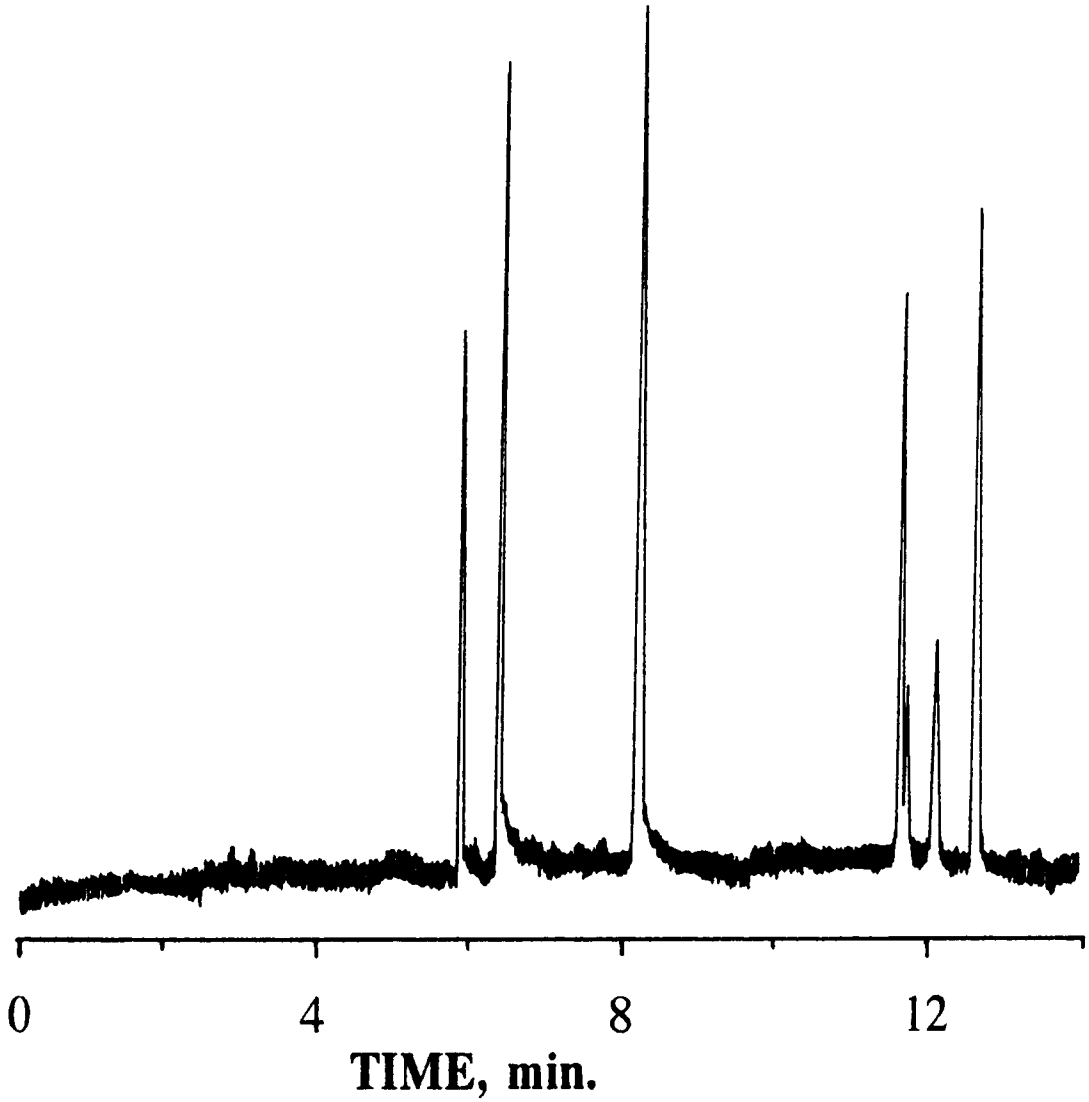

Figure 11 Separation of methyl-substituted BaP isomers. Solutes (in elution order) and conditions: BaP, 3-Me BaP, 5 Me-BaP, 7-Me BaP, 1 Me-BaP, 10 Me-BaP, 6 Me-BaP; 20 mM SDS and 15 mM γ-CD with 5 % 2-propanol.

as organic modifier.

It is logical that β-CD exhibits little effect on the retention of the isomers since its cavity dimension (~6.3 Å) would permit only partial inclusion complex formation with the "skinny end" of the BaP molecule. The hydrophobicity of the methyl-substituted BaP isomers is probably a significant solute descriptor. The relatively low k' for 7,10-diMe BaP with β-CD may result from a proper snug fit with the substituted "skinny end" of the isomer. Our molecular modeling studies resulted in a 7-Me carbon to 10-Me carbon distance of ~5.8 Å for this isomer. The derivatized cavity of the HPγ-CD results in relatively uniform interactions with the isomers. The narrow range in k' values (3.5 - 6.4) indicates that HPγ-CD is functioning largely as an organic modifier (although k's cannot be reduced to those low values using conventional organic solvents as modifiers). Conversely, the γ-CD cavity provides excellent discrimination between the isomers, with k' values ranging from 1.5 for BaP to 29 for 6-Me BaP. Duplication of the procedure described above for determining k' values resulted in the run 1 and run 2 data appearing in the table. While these k's are only approximate capacity factors, good repeatability in the measurements is evidenced by the closeness of the two runs (20, 31).

When coupled with efficiencies of greater than 10^5 plates/m (see below), successful separations of benzopyrene isomeric mixtures are possible (as demonstrated in Figures 10 and 11). The elution order of the 1-position isomers in Figure 10 is consistent with structurally related polarity considerations. The polar,

hydroxy-substituted isomer can hydrogen bond with the hydroxyl groups found on the lip of the CD when the "skinny end" of the BaP isomer is inserted into the cavity. Hence, association with the CD is expected to be stronger than the other 1-position isomers, and this is consistent with the observed elution order. It is much more difficult to predict the elution order of the Me-substituted isomers observed in Figure 11 based on general inspection of structure.

The high efficiency of these separations is somewhat surprising and may provide insights into the separation mechanism. When BaP is injected into a mobile phase without γ-CD, it elutes at t_m with an efficiency of about 8 x 10^4 plates/m. This modest efficiency for MECC may be limited by the adverse effects of micelle polydispersity. The contribution of micelle polydispersity to band dispersion in MECC increases in magnitude with increasing k' (20). The addition of CD greatly reduces k' and improves efficiency (e.g., N_{BaP} is about 2 x 10^5 plates/m in Figures 10 and 11). While this would be expected to reduce the polydispersity problem, it might be expected to create problems with slow mass transfer. Slow mass transfer should be particularly problematic if one of the phases involved in the mass transfer is the 5% 2-propanol mobile phase, in which BaP and its isomers are essentially insoluble. Consequently, the observed high efficiency provides strong evidence that the mass transfer process actually involves a direct exchange of BaP between micelle and CD, rather than the aforementioned stepwise mechanism.

molecular modeling considerations

data presentation

Data from the interaction energy matrices generated via implementation of the SYBYL molecular modeling procedures are presented in Table III. The starting position of the benzopyrene isomer was centered directly above the cavity with 10 Å between the centers' of mass (see Figure 12). From this position, the isomer was translated towards the CD cavity at 0.25 Å intervals to a final position 5 Å beyond the point at which the centers' of mass were aligned. At each translational position, the benzopyrene isomer was rotated 360° at 15° increments. In selected cases, the SYBYL DOCKING routine was used to locate interaction energy minima starting at given translational/rotational positions (see below). However, this was very time consuming and generally not employed.

Different initial orientations between benzopyrene and CD were used to generate energy matrices. Referring to Figure 12, showing structures for BaP and BeP, orientation 1 corresponds to an initial entry of positions 2 & 3 of BaP or 4 & 5 of BeP ("fat end") into the cavity, while orientation 2 corresponds to an initial entry of positions 8 & 9 of BaP or 10 & 11 of BeP ("skinny end"). Orientation 3 (used only for unsubstituted BaP and BeP) corresponded to a sideways approach (note that for BeP there are two equivalent approaches). In all these cases, the long axis of the benzopyrene is either parallel (orientation 1 & 2) or perpendicular (orientation 3) to the cavity axis during translation.

Table III. Normalized and actual solute/CD interaction energies (kcal/mol) for different orientations and methods of treating energy matrix values.

Compounds (in elution order)	Guest-Host Orientation[a] (average best five values w/o min.)					Composite using adjusted contour volume[c]
	Orientation 1		Orientation 2	Orientation 3	*Composite*[a]	
	w/o min.[b]	with min.[b]				
Figure 9						
BaP	(-9.9)	- - -	(-14)	(-5.8)x2	100[d] (-35.5)	- - -
BeP	(-5.4)	- - -	(-6.5)	(-7.6)x2	76 (-27.1)	- - -
Figure 10						
BaP	100[d] (-9.9)	100[d] (-19.4)	100[d] (-14.0)	- - -	100[d] (-23.9)	100[d] (-3204)
1-hyd BaP	63	89	92	- - -	78	65
1-eth BaP	67	81	83	- - -	75	27
1-Me BaP	54	84	87	- - -	71	69
Figure 11						
BaP	100[d] (-9.9)	- - -	100[d] (-14.0)	- - -	100[d] (-23.9)	100[d] (-3204)
3-Me BaP	81	- - -	94	- - -	88	111
5-Me BaP	81	- - -	84	- - -	83	78
7-Me BaP	105	- - -	37	- - -	71	46
1-Me BaP	54	- - -	87	- - -	71	69
10-Me BaP[e]	102[e]	- - -	103[e]	- - -	102[e]	111[e]
6-Me BaP[e]	100[e]	- - -	73[e]	- - -	87[e]	71[e]

a) Orientations and procedures for computing composite values are described in the text.
b) SYBYL DOCKING energy minimization was performed using the coordinates of the ten best (non-minimized) values as starting points. The average of the five best of these minimized values is reported.
c) Total contour volume is computed as the sum of all localized, non-minimized interaction energies lower than a cut-off value determined by the average value with solute/CD separation of 10.0 Å.
d) A normalized value of 100 is assigned to the average (or sum for the last column) negative interaction energy (in kcal/mol) of BaP.
e) 6-Me BaP and 10-Me BaP have independent minimized energies that are approximately 3 kcal/mol higher than the other isomers (~13 kcal/mol versus ~10 kcal/mol).

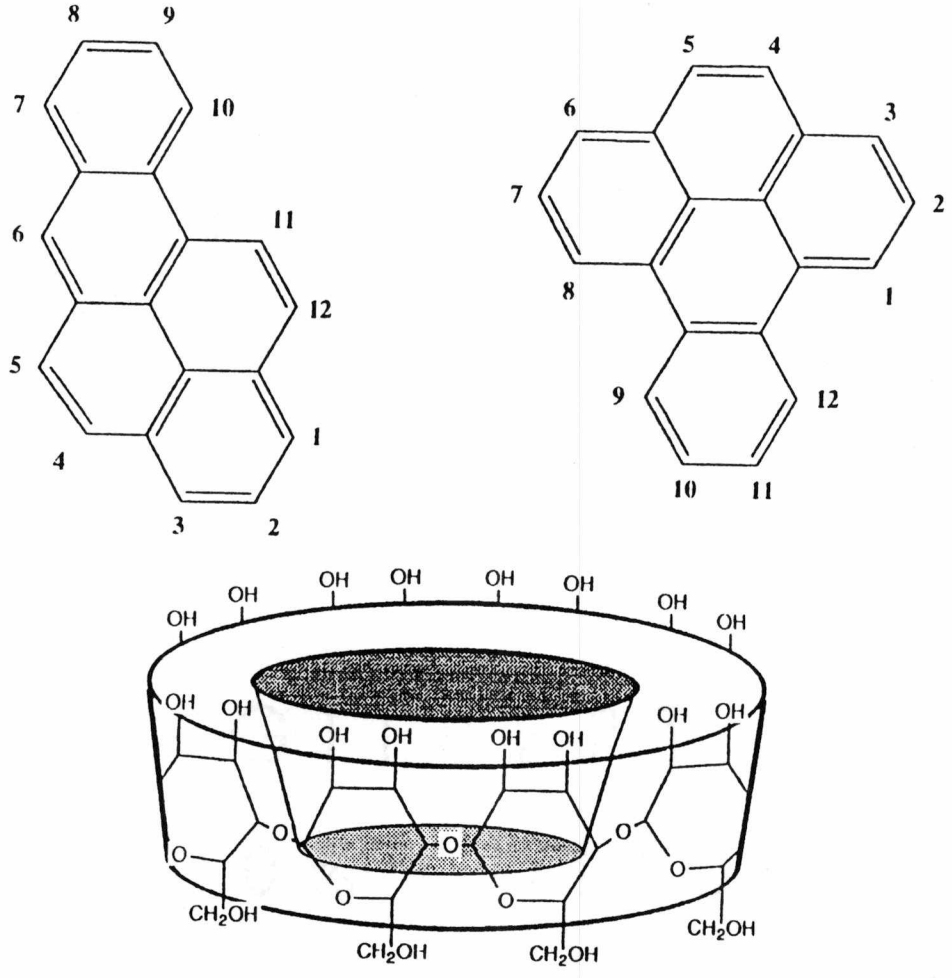

Figure 12 Depictions of BaP (on left), BeP, and γ-CD molecules.

Interaction energy in kcal/mol is reported for BaP and BeP; the former is assigned a value of 100. The interaction energies of the other isomers are based on this normalized 100 scale. Three benzopyrene/CD orientations and a composite sum of the interaction energies for those orientations are found in the table. Two approaches to representing the interaction energy data appear in the table. Most of the reported interaction energies are the averages of the five best (most negative) energy values in a given matrix. However, the last column is effectively the total volume of the contour formed by the energy values in the matrix (see Table III footnotes). The excessive time required to perform the interaction energy calculations with the computing system employed in this work necessitated certain omissions in the table. In particular, the sideways approach of the benzopyrene isomer (orientation 3) was performed only for the unsubstituted benzopyrene molecules. In the case of BeP there are two equivalent sideways orientations (see Figure 12), each yielding an average energy of -7.6 kcal/mol. While BaP does not possess the same symmetry with regard to this orientation, the SYBYL calculation yielded the same value of -5.8 kcal/mol for the two sideways approaches of that isomer.

scope of approach

The main focus of the molecular modeling work described herein was to (1) assign micropositional energy states (i.e., create the interaction energy matrices) and (2) properly interpret the significance of the states to establish correlations (if they exist) with benzopyrene isomer retention in CD-MECC. However, it is

instructive at this point to enumerate what is not considered in these computational studies of benzopyrene isomer elution behavior. In relation to Equation 10, elution order should correlate with trends in K_{CD-M}. The modeling that was performed provides energy (stability) information without consideration of solvation effects (i.e., isomers, γ-CD, and complexes are all considered to be in sterile environments for energy calculations). Moreover, entropy contributions to K_{CD-M} are not considered. The similar hydrophobicity, molar volume, and lack of symmetry of the solutes used in these studies provides some justification for these simplifications. It is expected that solvation effects (e.g., the expulsion of solvent or SDS monomer from CD cavity by the isomers) will be similar among the isomers and not contribute significantly to trends in K_{CD-M}. Entropy changes can be determined by measuring k' as a function of temperature (31). However, our apparatus is not equipped for such studies; furthermore, the entropy changes are also expected to be similar for these nonsymmetric BaP isomers.

A near-linear relationship was observed between retention and [CD]/[BaP] over a fairly wide concentration ratio range. A distinctive change in slope might indicate a change in the stoichiometry of complexation. Based on this study, CD and benzopyrene isomers were assumed to form one-to-one complexes in this work. The benzopyrene isomers all co-elute at t_m when γ-CD is not included in the mobile phase, indicating that K_M is very large. However, the last column of k' values in Table II (no CD; maximum tolerable % organic modifier) illustrates that there are significant

and detectable differences in k' (hence K_M) between some of the isomers. Nevertheless, we did not consider K_M when predicting elution order. As discussed above, the observed efficiency indicates that a stepwise process involving the K_M distribution (see Equation [10]) is probably not the principal separation mechanism. This is further supported by a lack of correlation between the high organic modifier and γ-CD k' data in Table II. Except for the early elution of BaP using both systems, the ordering of k' values are very different. The efficiency was very poor for the high organic modifier case. In fact, for certain isomers, it was obvious that concentrations required for detection exceeded or nearly exceeded solubility in the 22.5% acetonitrile mobile phase.

predictions of elution order

The correct elution order for the separation of BaP and BeP (see Figure 9) is predicted without considering orientation 3. However, when orientation 3 is not included, the disparity in composite interaction energies is very large, leading to the prediction that the isomers should be easily separated with the BeP exhibiting a very large k'. When the sideways orientation is considered, the BaP and BeP composite interaction energies are considerably closer in magnitude and more in line with the k' data in Table II and separation shown in Figure 9.

The potential significance of the sideways insertion of BeP into the cavity (i.e., partial inclusion complex formation) is fairly obvious from its structure. Such is not the case for the substituted BaP isomers and orientation 3 was not considered for those isomers.

The importance of considering both logical orientations ("fat" and "skinny end" approaches) for inclusion complex formation with the substituted isomers also can be seen from the data in Table III. Correct elution order is not predicted for the separations in Figures 10 and 11 based individually on orientation 1 or orientation 2 data. However, the composite (5 value average) is nearly correct for these separations. The two exceptions are the late eluting isomers, 10-Me BaP and 6-Me BaP (Figure 11). The SYBYL interaction energies predict a much stronger interaction with γ-CD than is indicated by their chromatographic behavior. Although we are uncertain as to the reason for the poor predictions for these isomers, we did note that they exhibited unusually large independent energies following use of the MINIMIZATION function of SYBYL (see Table III footnotes). Since these independent values are subtracted from the energy of the complex to determine the interaction energy, this would indicate a stronger interaction with γ-CD than would otherwise be predicted.

In principle, the SYBYL DOCKING routine could be employed to minimize the energy of the interaction complex using each of the translational/rotational positions in the energy matrices as starting points. Because this would require a prohibitive amount of computer time, a modified version of this approach was applied to the 1-positional isomers for orientation 1 (see Table III footnotes). For this selected case, the DOCKING routine rendered the computed interaction energies more similar and changed the ordering of the isomers. Clearly, the utilization of the minimization routine represents a refinement of the molecular modeling procedures used

in this work. However, this would require greater computing capability than exists with our system, but could yield better correlations between interaction energies and chromatographic behavior (see Chapter 8).

The presence of energy barriers that inhibit the formation of stable inclusion complexes could result in greater retention (less CD interaction) than would be predicted based on the five best energy values used in Table III. These considerations were also made by Arnold et al. concerning HPLC with cyclodextrins; noting that other researchers have observed alterations in elution order based on changes in flow rate and temperature (57, 77). If energy barriers are significant, the total contour volume (see last column in the table) might be expected to correlate better with chromatographic behavior, since that method of representation would include consideration of nearly all the energy values in the matrices generated in this work. As can be seen from the table, the correlation between elution order and composite interaction energy based on contour volume is weak at best.

The significance of energy barriers in influencing retention should also depend on the relative velocities of the chromatographic phases involved. The systems used to generate Figures 10 and 11 exhibited velocities for the mobile, γ-CD, and SDS-micellar phases of approximately 17, 17, and 3.8 cm/min, respectively. Thus, if solute mass transfer between phases involves separate CD/mobile phase exchange and mobile phase/SDS micelle exchange steps, energy barriers would not be important since there is no relative

velocity between CD and mobile phase. Conversely, if the solute is exchanging directly between micelle and CD (as hypothesized above), energy barriers could exert an influence on retention. The high separation efficiency achieved in this work indicates that significant energy barriers do not exist. Using the interaction energy matrices, we generated plots (similar to the one depicted in Figure 7) for both orientations of each isomer of number of rotational positions (out of 24 possible) versus translational position that have interaction energies above a reasonable cutoff value. A low number indicates stability of the complex throughout a complete rotation of the benzopyrene isomer. An inspection of these plots did not reveal any significant energy barriers that would inhibit insertion into the cavity to reach a position of maximum stability (i.e., the observed efficiency and the computational energy values are consistent in this regard).

In summary, high efficiency separations of hydrophobic benzopyrene isomers are shown to be possible using MECC with CD mobile phase additives. The ability to utilize molecular modeling techniques to make predictions concerning the effects of CDs on retention can greatly simplify methods development and provide insights into pertinent retention and band broadening mechanisms. Despite the complexity of the MECC system and the similarity between benzopyrene isomers, it is encouraging that elution order is predicted with fair accuracy. Only three orientations and two-dimensional positioning (translation and a perpendicular rotation) were considered in this work. Improvements in molecular modeling

systems (hardware and software) should reduce the time for computations and provide greater freedom with regard to solute/CD positioning. It is expected that this will enhance the predictive capabilities of this methodology.

Chapter 7
Cyclodextrin-Modified Capillary Electrophoretic Separations of Binaphthyl Enantiomers: Mechanistic and Molecular Modeling Studies

Introduction

Because of the extraordinary chiral recognition properties of BN derivatives in asymmetric synthesis reactions of organic compounds (78, 79) and metal-containing catalysts (80), methods of obtaining and characterizing optically pure supplies of BN enantiomers are needed. Previously, enantiomeric separations of BN compounds have been performed using micellar conventional (81) and microcolumn LC (82, 83), MECC (24), and LC employing CD bonded phases (84). These reports, as well as many others, offer only a brief, if any, explanation of the chiral separation process. However, if improved methods to separate BN enantiomers are to be created, a more rigorous understanding of chiral recognition mechanisms is essential.

Wren developed a mathematical model for enantio-selective separations using CD-CE and evaluated his model using several enantiomeric drugs as test solutes (85, 86). His model is based on the mobility of the free enantiomer (μ_f), the reduced mobility of the enantiomer/CD complex (μ_c), and the dynamic equilibrium between these species. In the simple case of a one-to-one interaction between binaphthyl (BN) and CD, a complexation constant (K_c) that

represents such a free solution equilibrium can be written as in Equation [11].

$$K_C = [CD\text{-}BN]/([CD]\,[BN]) \qquad [11]$$

He emphasizes the importance of maximizing the mobility difference, thus resolution, between enantiomers by optimizing the CD concentration. We concluded that his model, with slight modification, could be used to understand the CD-CE separation behavior of DNS-amino acids (see Chapter 8) and BN compounds (the results of the latter are described in this chapter).

The CD type and concentration that provide maximum enantiomeric resolution are a direct result of the strength of the inclusion complexes formed between each enantiomer and the CD. For this reason consideration of specific enantiomer/CD interactions, by way of molecular modeling, can be useful in determining experimental conditions that will provide chiral resolution in CD-CE. The work reported herein is unique in that the asymmetry in BN compounds is due to the rotational hindrance at the 1-1' bond rather than the presence of an asymmetric carbon atom, as was the case in the DNS-amino acid study (25).

While the main focus of this work was to resolve the enantiomers of BN compounds and use a modification of Wren's model to describe the separation behavior observed, results of molecular modeling studies are also reported. Although some

molecular modeling attempts were less informative than others, the findings of all efforts are described as a guide for future work.

Results and Discussion

separation behavior

As Wren reported (85), the observed mobility of an individual enantiomer (μ_{obs}) depends upon its distribution between free (f) and complexed (c) forms, as shown by Equation [12].

$$\mu_{obs} = \frac{\mu_f + \mu_c K_c[CD]}{1 + K_c[CD]} \qquad [12]$$

In order for enantiomeric resolution to be achieved in CD-CE, the mobility of each enantiomer of a pair must be different. This mobility difference ($\Delta\mu_{obs} = \mu_{obs,\,S} - \mu_{obs,\,R}$) is mainly a result of the differences in the equilibrium constants (K_c) associated with inclusion complex formation between each enantiomer of the analyte and the particular CD employed.

Wren's treatment considers μ_f and μ_c to be equal for the enantiomers of a particular compound. However, this study and the DNS-amino acid study (see Chapter 8) indicate that differences in μ_c exist within some pairs of enantiomers and can significantly influence enantio-selectivity; i.e., the diastereomers formed via complexation with CD do not always behavior identically in CD-CE.

For this reason, differences in μ_c must also be considered when describing mechanisms of enantiomeric separation by CDs. In this work, no effort was made to identify the S and R forms of the BN enantiomers; i.e., $\Delta\mu_{obs}$ is always taken to be positive and electropherograms indicate that the BN samples were roughly racemic mixtures.

Electropherograms comparing separation performance, with and without CDs added to the separation buffer, are seen in Figure 13. The elution order shown in Figure 13A (no CD case) is consistent with migration in opposition to a cathodic electroosmotic flow and the charges on these solutes; i.e., $BN(COOH)_2$ is ~-2, $BNPO_4$ is ~-1, and $BN(OH)_2$ is partially ionized at the pH (~9) that is employed. Inclusion complexation with a neutral CDs serves to reduce mobility and hence migration times. Obviously, the solute with the smallest mobility [$BN(OH)_2$] should, in general, exhibit the smallest changes in mobility due to CD inclusion. The electropherograms in Figures 13B-D involve 10 mM CD concentrations. Under these conditions, the smaller CDs, α and β, find utility in resolving the enantiomers of $BN(COOH)_2$ and $BNPO_4$, respectively. However, the separation buffer containing 10 mM γ-CD provided enantio-selectivity, complete or partial, for all three enantiomeric pairs.

It is convenient, yet not rigorous, to describe this behavior by comparing cavity size to molecular structure (note: structures are shown in Figure 13B). For instance, from molecular modeling studies the angle between the two naphthalene groups in the $BN(COOH)_2$ molecule is the largest of the three solutes. Therefore,

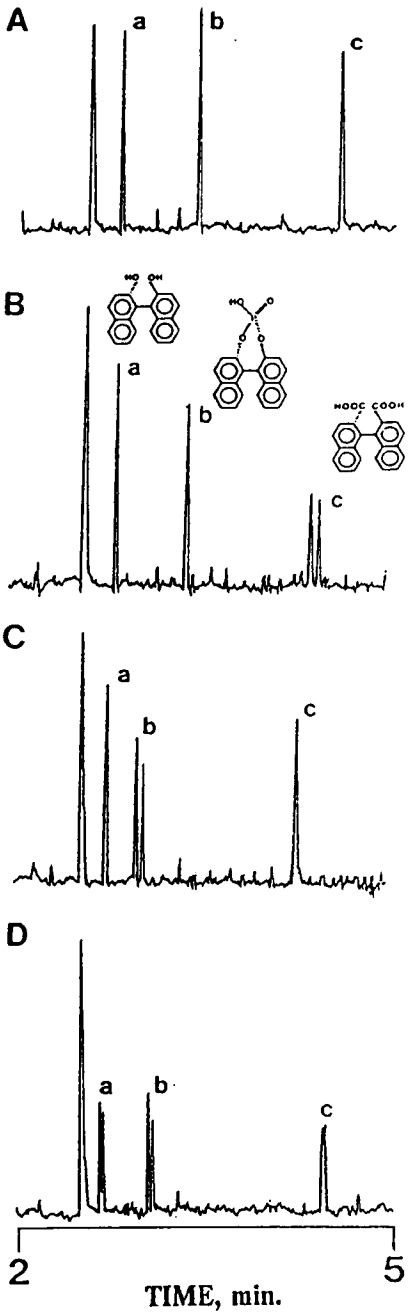

Figure 13 Separations of BN compounds employing various types of CDs. Solutes and conditions: t_o (unlabeled peak), $BN(OH)_2$ (a), $BNPO_4$ (b), and $BN(COOH)_2$ (c). In all cases, the separation buffer was pH 9 and CD was 10 mM in concentration. **A)** No CD present. **B)** α-CD. **C)** β-CD. **D)** γ-CD.

interaction with the CD cavity, which occurs by inclusion of one naphthalene group into the cavity, is possible even with the smallest CD, α-CD, since steric hindrance between the non-included naphthalene group and the lip of the CD is minimal. However, this type of logic does not hold true in attempting to explain the behavior of the other solutes, such as the $BNPO_4$ molecule, which has the smallest angle between naphthalene groups, but still interacts strongly with the medium-sized β-CD.

Even greater evidence that a discussion of cavity size verses molecular structure is inadequate comes from behavior observed when a large range of CD concentrations is employed. For instance, at a concentration of 10 mM α-CD there is no enantiomeric resolution of the $BNPO_4$ but at 30 mM α-CD, a resolution of 0.5 was observed. Similarly, the $BN(OH)_2$ enantiomeric pair shows no evidence of separation in Figure 13C, but was completely resolved when the β-CD concentration was increased to 30 mM. In some cases, such as that of $BN(OH)_2$ with γ-CD (see Figure 13D), use of greater concentrations of CD (20 mM and above) actually degrades the enantiomeric resolution. This can occur when differences in K_c values between the enantiomers are overwhelmed by large CD concentrations, and both enantiomers are nearly completely complexed.

The above examples indicate the need for a comparison of enantiomer mobility to CD concentration in order to accurately describe separation behavior. Using the TableCurve plotting program (see Chapter 4), each enantiomer's mobility was plotted verses CD

concentration for all three CDs employed. Figure 14 contains plots resulting from the separations performed using γ-CD. For these plots, as well as those generated with data from the other two CDs, the plotting program provided an equation of fit in the form of $y = (a + cx)/(1 + bx)$ which matches that of Equation [12]. The quality of the fit of this data to Equation [12] is reflected in correlation coefficients that averaged 0.983, and the fact that in each case the aforementioned equation provided the best fit from a TableCurve field of over 200 linear equations. The values of a, b, and c/b provided by the plotting program give rise to values of μ_f, K_c and μ_c, respectively, and can be found in Table IV. For comparative purposes, values of $\mu_{f,ex}$, experimentally determined without CD in the separation buffer, are also presented in the table. It is encouraging that these values are in strong agreement with values of μ_f provided by the plotting program.

Upon inspection of the broken lines for $BNPO_4$ in Figure 14, a convergence in the plotted data is observed. It seems peculiar that there are measurable differences in the values of μ_c for the $BNPO_4$ enantiomers (see Table IV), which normally indicates enantiomeric resolution will occur at high CD concentrations, and yet there is no resolution at γ-CD concentrations of 30-40 mM. This behavior is explained by noticing that value of μ_c for the earlier eluting $BNPO_4$ enantiomer is larger than that of the later eluting enantiomer and that the K_c values follow this same pattern. K_c and μ_c values such as these can function to cancel each other out thus negating enantiomeric resolution; i.e., the enantiomer with the larger K_c

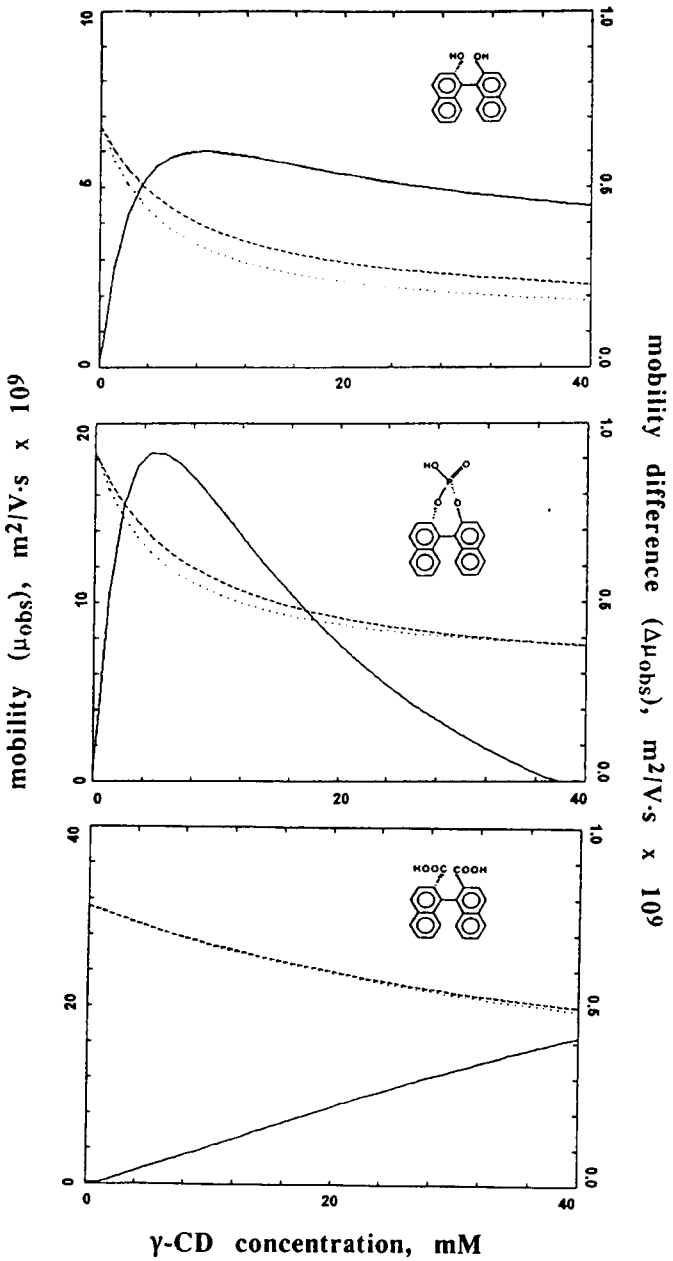

Figure 14 Plots of mobility and mobility difference versus γ-CD concentration for $BN(OH)_2$, $BNPO_4$, and $BN(COOH)_2$. Dotted and dashed lines correspond to mobilities of enantiomers (left axis) and solid line corresponds to mobility difference (right axis).

Table IV. BN mobility and Kc data.

	$\mu_{f,ex}$ x10^9 [a]	μ_f x 10^9 [b]	μ_c x 10^9 [c]	K_c [d]
α-CD				
R&S $BN(OH)_2$	6.17	6.16	2.06	13.5
	6.17	6.16	2.06	13.5
R&S $BNPO_4$	17.9	17.8	1.36	8.89
	17.9	17.8	6.73	14.3
R&S $BN(COOH)_2$	31.1	31.0	4.85	13.7
	31.1	30.97	5.99	11.5
β-CD				
R&S $BN(OH)_2$	7.38	7.36	1.23	72.9
	7.38	7.34	1.30	55.2
R&S $BNPO_4$	18.6	18.2	6.41	221
	18.6	18.3	7.00	180
R&S $BN(COOH)_2$	33.0	31.9	11.9	35.9
	33.0	31.9	11.9	35.9
γ-CD				
R&S $BN(OH)_2$	6.88	6.71	1.24	187
	6.88	6.70	1.51	132
R&S $BNPO_4$	18.5	18.3	6.18	183
	18.5	18.3	5.38	120
R&S $BN(COOH)_2$	31.3	31.2	5.02	20.1
	31.3	31.2	6.52	21.0

a) $\mu_{f,ex}$ is the mobility ($m^2/V{\cdot}s$) of free BN measured without CD.

b) μ_f is the mobility ($m^2/V{\cdot}s$) of free BN calculated using constants derived from plotting program fit of Equation 12.

c) μ_c is mobility ($m^2/V{\cdot}s$) of BN/CD complex calculated as in (b).

d) K_c is the complexation constant for BN/CD complex calculated as in (b).

value, hence a tendency to elute earlier, also has a higher μ_c value, hence a tendency to elute later. If γ-CD concentrations were not solubility limited, one would expect that very high concentrations would again produce a $BNPO_4$ separation with a reversal of enantiomer elution order.

The solid lines in Figure 14 represent the effect of γ-CD concentration on mobility differences between the BN enantiomers. The plot for $BN(OH)_2$ exhibits a broad optimum which spans the concentration range while a sharp optimum at low concentration is observed for $BNPO_4$. If there are no differences in μ_c for the enantiomers, large K_c values such as for $BN(OH)_2$ and $BNPO_4$ (see Table IV) result in a distinct optimum $\Delta\mu_{obs}$ at low CD concentration. The plot for $BN(OH)_2$ deviates from this behavior because of differences in μ_c and the plot for $BNPO_4$ exhibits this behavior despite differences in μ_c for the reason discussed above. In the case of $BN(COOH)_2$, there is no optimum value of $\Delta\mu_{obs}$ over the CD concentration range studied. Instead, $\Delta\mu_{obs}$ continues to increase with γ-CD concentration, which is consistent with the very small value of K_c for this compound (see Table IV).

molecular modeling

Molecular modeling can assist in determining the type of CD that will lead to maximum resolution for a particular enantiomeric pair. It can also provide insight into mechanisms that are responsible for enantiomeric discrimination. In a separate study (see Chapter 8), it was found that a simple statistical mechanical

approach of treating interaction energies resulted in a good correlation between molecular modeling results and enantiomer elution order (25). However, in that study, the solutes (DNS-amino acid enantiomers) were geometrically similar. For this reason, it was possible to compare the separation behavior of different amino acid enantiomers, in relation to a particular CD, and find a correlation with molecular modeling data. Since the BN enantiomers studied herein are not as structurally similar as were the DNS-amino acids, a correlation between separation results and molecular modeling cannot be found in the same manner. However, the molecular modeling does permit comparisons of the effects of different CDs on enantio-selectivity for the BN compounds taken individually (see below).

In the modeling studies that lead to the data in Table V, the centers of the BN enantiomer (defined as the center of the naphthalene ring to be included) and CD were initially positioned 6.0 Å apart and translated towards each other in increments of 0.25 Å to a final separation of 2.0 Å (at which energetically unfavorable steric interactions existed). At each translational distance, the BN enantiomer was rotated a total of 360° by increments of 5.0°. In some instances, the MINIMIZE function of SYBYL was employed starting at selected of these positions. In other situations, the solute/CD complex was solvated prior to minimization. The DISPLAY H-BONDS function of SYBYL was used to identify hydrogen bonds in some complexes. Further details regarding molecular modeling procedures and calculation of Z values are found in Chapter 4.

Table V compares the molecular modeling results with experimentally determined K_c and μ_c values. In principle, when comparing the separation behavior of the three CDs for a given BN compound, trends in ln Z should follow K_c values and indicate the strength of the BN/CD interaction. Similarly, relative differences in Δln Z (second column in the table) should follow relative differences in ΔK_c (fourth column) and indicate the degree of enantioselectivity. It is encouraging that except for $BN(OH)_2$ with γ-CD, the ordering of ln Z and relative Δln Z values do follow the orders for K_c and relative ΔK_c values. The lack of agreement for $BN(OH)_2$ could indicate the mechanism (or orientation) of the interaction of that BN compound is different with γ-CD than for the two other CDs. It is important to note that the modeling data do not provide information concerning μ_c, which is shown in this report to also influence separation performance.

The modeling work would have practical utility if it facilitates picking optimum separation conditions (e.g., choosing the best type and concentration of CD). As an example, the modeling data for $BN(COOH)_2$ works well in this regard. Because of a large relative Δln Z value and a modest ln Z value (see Table V), the modeling data point toward using an intermediate concentration of α-CD for optimum separation of the $BN(COOH)_2$ enantiomers. This is consistent with experimental results; e.g., consider the separations shown in Figure 13 and the fact that a distinctive optimum was observed at intermediate concentration in a plot of $\Delta\mu_{obs}$ versus [α-CD]. The poorest choice of CD should be γ-CD since it provides the

Table V. BN molecular modeling results.

	ln Z_{av} [a]	Δln Z / ln Z_{av} (x100)	$K_{c\ av}$ [b]	ΔK_c / $K_{c\ av}$ (x100)	$\mu_{c\ av}$ x 10^9 [c]	$\Delta \mu_c$ / $\mu_{c\ av}$ (x100)
α-CD						
$BN(OH)_2$	18.8	6.38	13.5	0	2.06	0
$BNPO_4$	11.3	37.8	11.6	47.0	4.05	133
$BN(COOH)_2$	15.2	20.4	12.6	17.4	5.42	21.0
β-CD						
$BN(OH)_2$	27.1	11.8	64.0	27.7	1.26	5.79
$BNPO_4$	25.5	6.67	201	20.8	6.71	8.91
$BN(COOH)_2$	26.0	2.69	35.9	0	11.9	0
γ-CD						
$BN(OH)_2$	22.4	8.93	160	34.0	1.38	19.4
$BNPO_4$	23.5	8.09	152	41.1	5.78	13.8
$BN(COOH)_2$	22.2	0.901	20.6	4.11	5.77	26.0

a) ln Z_{av} is natural log of the average partition function, calculated using Equation [8] from interaction energy matrix, for each enantiomer pair. Δln Z is the difference in ln Z for a pair.

b) $K_{c\ av}$ is the average complexation constant, for each enantiomer pair, determined by using the TableCurve plotting program. ΔK_c is the difference in K_c for a pair.

c) $\mu_{c\ av}$ is the average mobilities ($m^2/V \cdot s$) of the completely complexed BN, for each enantiomer pair, determined by using the TableCurve plotting program. $\Delta\mu_c$ is the difference in μ_c for a pair.

smallest relative Δln Z value. The fact that this is not seen in Figure 13 (i.e., γ-CD works better than β-CD) is probably due to a very large value of $\Delta\mu_c$ for $BN(COOH)_2$ with γ-CD. In fact baseline resolution is observed at 40 mM γ-CD. Thus molecular modeling falls short of completely describing enantio-selectivity in CD-CE. Similar predictions can be made from the modeling data in Table V for the $BNPO_4$.

In an attempt to extend the use of molecular modeling to determine separation mechanisms in CD-CE, several studies, beyond the statistical mechanical approach described above, were performed. These included inspection of several complexes for hydrogen bonding and evaluation of solvation and minimization on molecular modeling calculations.

Enantioselectivity by CDs is based on the inclusion of the hydrophobic region of a molecule into the CD and hydrogen bonding between portions of the guest molecule that are in proximity to the hydroxyl groups surrounding the opening of the cavity (87). Therefore, the number and energy of hydrogen bonds in the various BN/CD complexes was thought to possibly provide a correlation with the separation behavior observed. However, inspection of several of the lowest energy (most favorable) BN/CD complexes for hydrogen bonds resulted in no strong correlation.

As described above, the MINIMIZE function of the modeling program can be used to find the best geometrical conformation of a particular complex. In related work involving chiral separations of DNS-amino acids (see Chapter 8), minimization of the lowest energy

complexes correctly predicted the observed elution order. Furthermore, the minimized DNS-amino acid/CD complexes were not unreasonably distorted (due to the nearly complete inclusion of the DNS group into the CD). In the case of BN/CD complex formation, only a small portion of the BN is included into the CD. Attempts to minimize these complexes resulted in final structures that were quite distorted. For example, one or two glucopyranose units of the CD were perpendicular, rather than the normal parallel, to the cavity's opening. Essentially, minimization of an unsolvated BN/CD complex resulted in a structure that, although computed to be energetically most favorable, would not be expected to occur. This is clearly a limitation of the modeling software used in these studies. We found that solvating the complex with water prior to minimization kept unreasonable distortions from occurring but was extremely time consuming and only explained the separation behavior for some BN/CD combinations.

It has been shown that enantiomeric resolution of $BN(OH)_2$, $BNPO_4$, and $BN(COOH)_2$ is strongly dependent on the type and concentration of CD employed. Therefore, optimization of separation conditions is essential to obtain maximum enantiomeric separation for each of these chiral compounds. The optimization process can be simplified using BN/CD interaction energies, calculated through molecular modeling, as a guide.

Chapter 8
Cyclodextrin-Modified Capillary Electrophoretic Separations of Derivatized Amino Acid Enantiomers: Mechanistic and Molecular Modeling Studies

Introduction

The resolution of racemic mixtures of optical isomers is becoming increasing important in analytical separations. Not only is the problem experimentally challenging, but the optical purity of these isomers is of critical importance in areas such as the production of therapeutic drugs. Chemical analysis by preparation and physical separation of diastereomers has been supplanted by chromatographic and electrophoretic separation using chiral stationary phases and separation buffer adducts. In this regard, the exceptional efficiency, hence resolving power, of CE, and the related technique MECC, renders those methods valuable for enantiomeric separations. Because the choice of enantio-selective reagent is often based largely on trial and error, the ease and speed with which CE/MECC separation buffer composition can be altered to influence selectivity is a distinct and important advantage.

Inclusion complex formation with CDs modifies retention by reducing the electrophoretic mobility of charged solutes in CE (note: MW of neutral γ-CD is 1297) and by inhibiting the association of neutral solutes with the micellar phase in MECC (71). Most of the reports of CD use in CE present observations concerning the effects of CD type and concentration on retention, but only briefly discuss

mechanisms for enantio-selectivity. In one exception, Wren developed a mathematical model (see details in Chapter 7) for enantio-selective separations using CD-CE (85, 86), that can be reasonably applied to this work with DNS-amino acids. In the simple case of a one-to-one interaction between amino acid (AA) and CD, a complexation constant (K_c) that represents such a free solution equilibrium can be written as in Equation [13].

$$K_C = [CD\text{-}AA]/([CD]\,[AA]) \qquad [13]$$

In principle, molecular modeling techniques can assist in computing the forces that determine the magnitude of K_c and, perhaps more importantly, determine if those forces significantly involve the chiral portions of the enantiomer and CD. Thus, molecular modeling techniques offer the promise of computationally providing predictions and a better fundamental understanding concerning the effects of solute/CD inclusion complexation on retention behavior in CE/MECC. The studies described herein concern the applicability of both the aforementioned Wren's mathematical model for enantio-selective separations and this molecular modeling system to CD-CE separations of DNS-amino acid enantiomers.

Results and Discussion

retention model

The observed mobility of an amino acid enantiomer (μ_{obs}) will depend on its distribution between free and complexed forms which is governed by Equation [13]. By analogy to the treatment of Wren, this yields the expression in Equation [12] in Chapter 7.

Enantiomer resolution requires that there be a difference in observed mobility between D and L enantiomers as given by Equation [14].

$$\Delta\mu_{obs} = \mu_{obs,\,D} - \mu_{obs,\,L} \qquad [14]$$

As described in Chapter 7, Wren's treatment considers μ_f and μ_c to be equal for the enantiomers and non-zero values for $\Delta\mu_{obs}$ are attributed to distinctive values of K_c (i.e., $K_{c,D}$ and $K_{c,L}$ are not equal). While we observe no difference in μ_f between enantiomers, our results (see below) indicate that μ_c is not the same for the D and L enantiomers of certain amino acids. Thus, $\Delta\mu_{obs}$ is primarily influenced by differences in K_c, but differences in μ_c may also contribute to enantio-selectivity.

The separation performance that is possible in this application is demonstrated in Figure 15 for β-CD and for low, mid, and high concentrations of γ-CD. Several significant observations can be made with regard to the figure. First, the retention time of acetone (large early eluting peak) increases at large γ-CD concentrations.

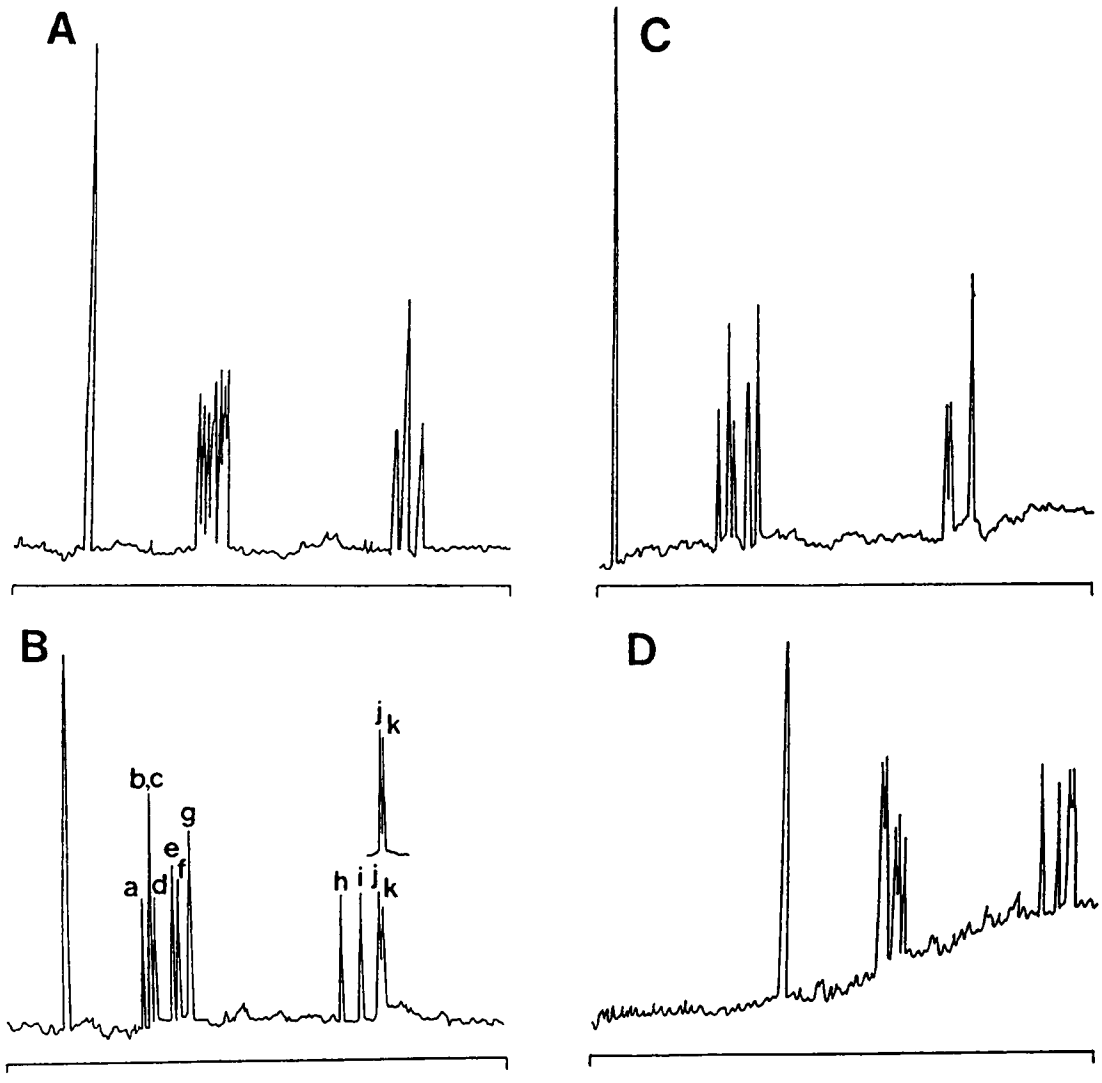

Figure 15 Separations of DNS-amino acids employing various types and concentrations of CDs. Solutes and conditions: t_o (unlabeled peak), D-Leu (a), L-Leu (b), D-Val (c), L-Val (d), D-Thr (e), L-Thr (f), D and L-Ser (g), D-Glu (h), L-Glu (i), D-Asp (j), and L-Asp (k). **A)** 10 mM β-CD. **B)** 10 mM γ-CD. **C)** 1 mM γ-CD. **D)** 60 mM γ-CD. Axis on all electropherograms spans 3 to 7 min.

We assumed in this work that this signaled a reduction in electroosmotic flow rather than the association of acetone with the CD. The adherence of the mobility data to the derived model (see below) when acetone is used to mark column void time and compute electroosmotic velocity reinforces this assumption. The best overall separation in the figure occurs for the 10 mM γ-CD separation buffer. At higher concentrations, most of the early eluting enantiomers "bunch-up" (see Figure 15D). Even at 10 mM γ-CD, the L Leu (b) and D Val (c) co-elute. Actually, a separation buffer that was 5 mM in both β- and γ-CD (not shown in the figure) resolved b and c and provided the best overall resolution. The electropherograms in Figure 15 illustrate that for complex mixtures of enantiomers, system optimization must consider both general and enantio-selective elution behavior. Simplex methods, which we have applied to the optimization of solvent gradients in MECC (88), may find utility in those situations.

In general, the γ-CD provides for better resolution of the enantiomers. The one exception is Ser for which it is only possible to achieve partial resolution with an optimized concentration of β-CD. The overall better performance for the γ-CD may be attributed to a more appropriate fit of the DNS label into its larger CD cavity (see Figure 16). The late eluting doubly charged amino acids (h through k) are difficult to resolve and require strict optimization of γ-CD concentration. In this regard, the superior efficiency afforded by laser fluorometric detection and narrow i.d. capillaries (21, 71, 89) is important in resolving the enantiomers of Asp (see insert in

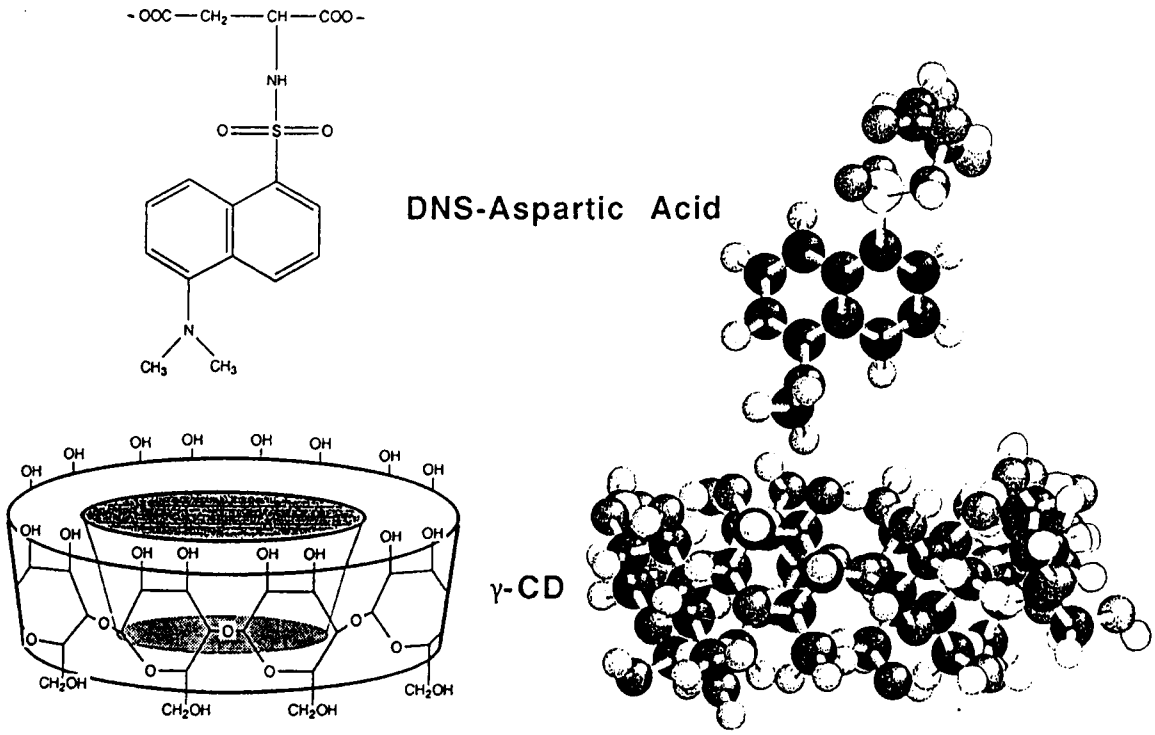

Figure 16 Depiction of D-Asp and γ-CD structures. SYBYL molecular modeling images (ball and stick representations) on right.

Figure 15B obtained using a 25 μm i.d. capillary).

Figure 17 and Table VI present data from detailed studies of the effect of γ-CD concentration on the mobility of the tested DNS-amino acids. The figure contains μ_{obs} for D-Asp and L-Asp over the range 0.5 - 100 mM γ-CD. It is reassuring that the plotting program (see Chapter 4) used to generate the curves provided a reliable fit using an equation of the form of Equation [12] (i.e., $y = (a + cx)/(1 + bx)$). This was true of all the tested amino acids. The values of $\mu_{f,exp}$ for Asp and the other amino acids that appear in the table were determined without CD in the separation buffer. The values of μ_f, μ_c, and K_c were computed from the constants supplied by the TableCurve plotting program through utilization of retention (mobility) data covering the full range of γ-CD concentrations. The last two columns of the table provide information on separation performance as expressed by mobility and complexation constant ratios for the enantiomers. Based on the reasonable correlation coefficients obtained (see Figure 17 caption), and about a 10% discrepancy between the $\mu_{f,exp}$ and μ_f values in Table VI, we feel that the enantiomer mobility ratios for Leu, Val, Thr, and Ser are not significantly different from 1.0. In those cases, when separation occurs (not observed for Ser with γ-CD) it is the result of differences in K_c. This is consistent with Wren's model. Conversely, there appears to be a significant difference in the mobilities of the enantiomers of the doubly charged amino acids; the mobilities of the D enantiomers of Glu and Asp are determined to be 36% and 45% greater, respectively, than that of the L enantiomers.

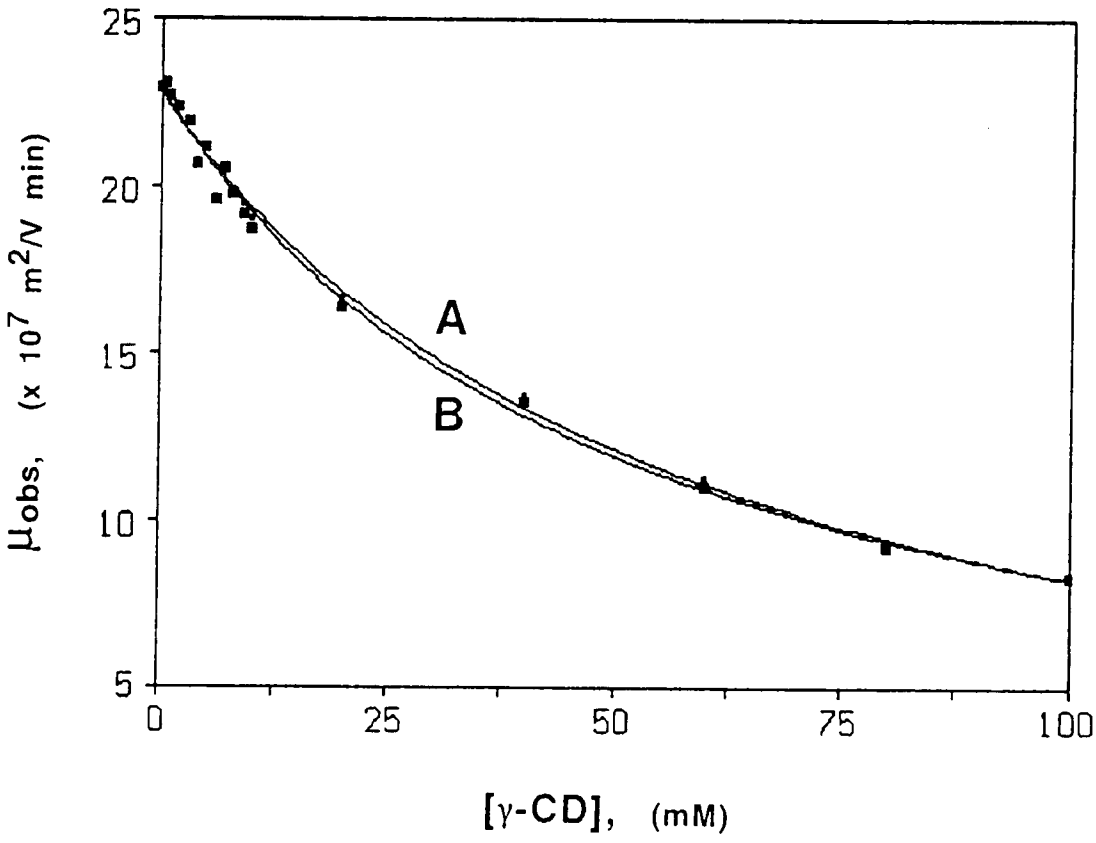

Figure 17 Plot of (A) L and (B) D-Asp observed mobility as a function of γ-CD concentration. Curves based on Equation 12 (Chapter 7) yielding correlation coefficients of 0.994.

Table VI. DNS-amino acid mobility and K_c data.

DNS-amino acid	$\mu_{f,\,exp}$ [a]	μ_f [b]	μ_c [c]	$\mu_{c,D}/\mu_{c,L}$	$K_{c,D}/K_{c,L}$ [d]
D Leu	12.0	10.5	2.76	1.08	1.12
L Leu		11.1	2.57		
D Val	12.2	11.3	2.61	1.08	1.14
L Val		11.6	2.43		
D Thr	12.5	12.4	2.02	1.08	1.21
L Thr		12.5	1.87		
D Ser	13.0	13.1	1.75	1.00	1.00
L Ser		13.1	1.75		
D Glu	22.3	22.3	3.42	1.36	1.28
L Glu		22.4	2.52		
D Asp	22.9	23.1	2.45	1.45	1.13
L Asp		23.0	1.69		

a) $\mu_{f,exp}$ is mobility (x 10^7 m^2/V min) of free amino acid measured without CD.

b) μ_f is mobility (x 10^7 m^2/V min) of free amino acid calculated by using constants derived from plotting program fit of Equation [12].

c) μ_c is mobility (x 10^7 m^2/V min) of amino acid/CD complex calculated as in (b).

d) $K_{c,D}/K_{c,L}$ is ratio of the complexation constants of D and L enantiomers calculated as in (b).

We are not clear as to the nature of this somewhat surprising mobility effect. However, it is possible that the net charge or solvation sphere of the CD-complexed enantiomers of Glu and Asp are not identical, as is the case in free solution, and this provides for enantio-selective differences in mobility.

Figure 18 contains plots of observed enantiomer mobility differences versus γ-CD concentration for Leu and Asp. The former amino acid exhibits a rather sharp optimum at low concentration while the latter shows a rather broad optimum at higher concentration. This is consistent with data used to generate Table VI. The optimum CD concentration should be inversely proportional to the value of K_c (85). These values are 80 and 24 for Leu and Asp, respectively (averages for the D and L enantiomers). The broad maximum for Asp is also consistent with the observed difference in the mobilities of its D and L enantiomers which, unlike the Leu, would favor complete complexation. The insert in Figure 18 provides optimum CD concentration and $\Delta\mu_{obs}$ data for the amino acids tested. The critical and distinctive optima with regard to CD concentration point toward compromises in conditions, or solvent gradient approaches (88), when mixtures of amino acids are involved.

molecular modeling

Previous efforts involved the translation and rotation (at relatively large increments) of benzopyrene substitutional isomers into and around the cavity of γ-CD (see Chapter 6) (71). Interaction

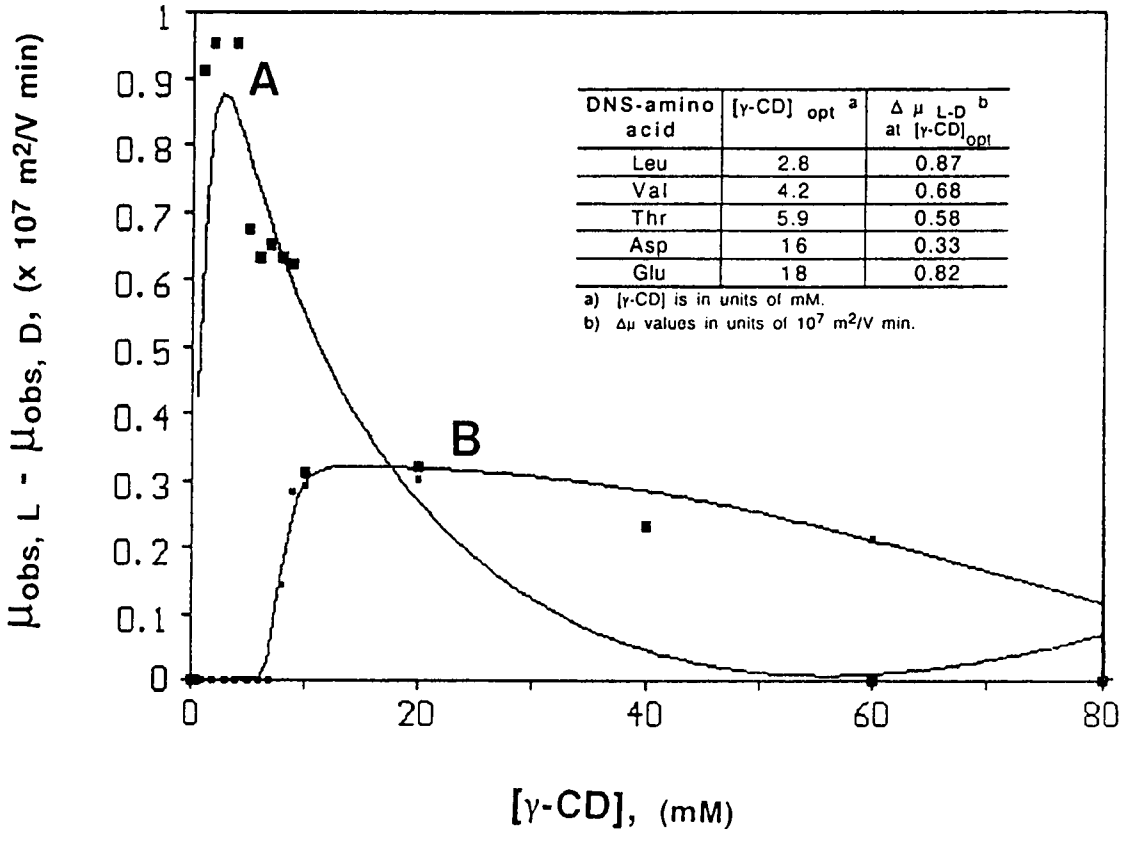

DNS-amino acid	[γ-CD] opt [a]	Δ μ L-D [b] at [γ-CD]opt
Leu	2.8	0.87
Val	4.2	0.68
Thr	5.9	0.58
Asp	16	0.33
Glu	18	0.82

a) [γ-CD] is in units of mM.
b) Δμ values in units of 10^7 m^2/V min.

Figure 18 Plot of (A) Leu and (B) Asp observed mobility difference as a function of γ-CD concentration.

energies were calculated by using the SYBYL software, without minimizing the complex (geometric optimization), at each position. A relatively large interaction space was sampled in generating rather large interaction energy matrices. Two logical orientations (approaches) of the benzopyrene isomers were considered. Correct elution order was predicted for most of the benzopyrene isomers based on the average of the five lowest energies in the matrices (both orientations considered) (71). This same approach (i.e., large matrix, large increments, no minimization) was initially applied to the DNS-amino acid enantiomers. However, we considered only one orientation, that involving the translation of the relatively hydrophobic DNS group into the cavity, leaving the amino acid portion to interact primarily with the lip. The results appear in the first column of Table VII. The average of the five lowest (most negative interaction energies) do not correctly predict the first elution (stronger interaction) of the D enantiomer in two of three cases. This was disappointing in that assumptions applied in our more successful benzopyrene work (i.e., ignoring entropy effects) were expected to be more appropriate for enantiomer pairs. Minimizing the complex (via the SYBYL MINIMIZATION routine) using the positions of the five best energies in the matrices as starting points did not improve predictions, as shown in the second column of the table.

The third and fourth columns of the table show the results of a more successful approach. The large matrices were inspected to determine a short translational range over which strong interactions

Table VII. DNS-amino acid molecular modeling results.

DNS-amino acid [a]	5 lowest[b] w/o min. large matrix	5 lowest[c] w/ min. large matrix	5 lowest[d] w/ min. small matrix	Z [e] small matrix	$K_{c,D}$ / $K_{c,L}$ [f]
D Leu	-14.6	-51.7	-62.0	1.1×10^{48}	1.12
L Leu	-14.7	-47.7	-59.2	2.2×10^{44}	
D Ser	-14.1	-47.5	-68.3	8.9×10^{50}	1.00
L Ser	-14.5	-49.6	-66.1	2.6×10^{49}	
D Asp	-16.1	-50.9	-69.1	3.2×10^{51}	1.13
L Asp	-15.0	-62.0	-60.5	1.8×10^{46}	

a) The minimized energies (kcal/mol) of free DNS-amino acid enantiomers of Leu, Ser, and Asp are 14.3, 14.2, and 19.8, respectively.

b) Reported values are an average of the 5 lowest, non-minimized interaction energies resulting from energy matrix which considered large tran/rot space.
Translation: beginning, -10 Å, ending, +1.0 Å, increment, 0.25 Å
Rotation: beginning, 0°, ending, 360°, increment, 10°

c) Reported values are an average of the interaction energies resulting from minimizing starting at each of the 5 lowest energy postions found using large matrix (see(b)).

d) The values reported are an average of the 5 lowest interaction energies resulting from energy matrix which considered a small translational/rotational space and minimized at each position.
Translation: beginning, -1.5 Å, ending, +0.5 Å, increment, 0.50 Å
Rotation: beginning, 0°, ending, 90°, increment, 5°

e) Reported values of Z calculated from small matrix (see (d)) by using Equation [8].

f) K_c data copied from Table VI.

were expected. Next, a smaller rotational increment but only over a quarter of the full rotation was chosen (see table footnotes). The MINIMIZATION routine was applied at each of these positions. The five lowest energies from these relatively small matrices correctly predicted D/L elution order. Similar success was obtained by using all the values in the small matrix to compute the partition function (Z) by using Equation [8]. The relative differences in Z for the enantiomer pairs also seem to correlate with the K_c ratios (last column) transposed from Table VI. Although comparisons between the Z values of different amino acids should be made with care, it appears that the difficulty in separating the enantiomers of Ser does not reside in a poor interaction with the γ-CD (note large Z value), but in a lack of enantio-selectivity. In fact, the K_c value of Ser falls between the values previously given for Leu and Asp (see discussion concerning Figure 18).

A major drawback to this small matrix but total minimization approach is that the generation of each matrix required over 24 hours of computational time on our system. This is the reason for considering only γ-CD and three of the amino acids. Obviously, improvements in pertinent computer software and hardware could dramatically reduce the time required for these computations.

Chapter 9
Cyclodextrin Distribution Capillary Electrochromatographic Separations of Polycyclic Aromatic Hydrocarbons

Introduction

A substantial limitation of CE is its inability to separate neutral species. Because of the preponderance of neutral compounds in samples of biological, environmental, and industrial origin, this limitation is particularly significant to current CE technology. Neutral compounds can be separated if they acquire an effective mobility due to association with charged separation buffer additives such as ionizable CDs.

Terabe and co-workers first demonstrated that carboxylated-CDs can function in a manner similar to negatively charged micelles (as the secondary phase described above) for separations of water soluble neutral compounds (90). More recently, enantiomeric separations of water soluble compounds (mostly chiral drugs) have been facilitated using separation buffers containing charged CDs (91-93). Migration behavior depends on the ionic state of the drug and the magnitude of electroosmotic flow (91).

The work described in this chapter differs from the approaches discussed above in two significant regards. First, the separation of hydrophobic PAH molecules that are essentially insoluble in the separation buffer is demonstrated. Second, the electrokinetic chromatography buffer system is comprised of a secondary phase

that is charged CD and a primary phase that is neutral CD, rather than separation buffer as with other approaches; i.e., the separation buffer functions solely as a carrier fluid. Separations are based on a differential distribution between these distinct CD phases. Hence, this CE variant is referred to as CDCE. A preliminary evaluation of the technique is presented that focuses on efficiency, selectivity, and system retention characteristics, with an emphasis on comparisons with MECC.

Results and Discussion

By analogy with the expressions derived by Terabe (see Chapter 2) for capillary electrokinetic chromatography (31, 90), the values for resolution (R_s) and k' in CDCE are given by Equations [15] and [16], respectively.

$$R_s = \frac{N^{1/2}}{4} \cdot \frac{\alpha - 1}{\alpha} \cdot \frac{k'_2}{1 + k'_2} \cdot \frac{1 - t_{ne}/t_{ch}}{1 + (t_{ne}/t_{ch})k'_1} \qquad [15]$$

$$k' = \frac{t_r - t_{ne}}{t_{ne}(1 - t_r/t_{ch})} = \frac{V_{charged}}{V_{neutral}} \times K_D \qquad [16]$$

In these equations, α is a selectivity factor (k'_2/k'_1), $V_{charged}/V_{neutral}$ is the CD volume phase ratio for the system, and K_D is the distribution coefficient of the solute between the CD phases.

The times appearing in the equations, t_{ne}, t_{ch}, and t_r, are the effective retention times of the neutral CD, charged CD, and injected solute, respectively. Because the charged CD sample used in this work is very polydisperse (see below) and, unlike normal micelles, is a "fixed" organized assembly (i.e., does not exchange between its various derivatized forms), the value of t_{ch} is not well-defined. Nevertheless, we have used the t_r of the PAH anthracene, in a system without neutral CD, as a means to determine t_{ch}. This is based on the observation that without neutral CD in the running buffer, the effective electrophoretic mobility of anthracene did not change as the concentration of CMβ-CD was varied from 1 to 15 mM (i.e., anthracene appears to have a very large inclusion complexation constant with CMβ-CD). This mobility is taken to approximate an aggregate electrophoretic mobility of the many forms of CMβ-CD. The CMβ-CD mobility obtained in this manner is assumed to be constant and is used to calculate t_{ch} for certain of the CDCE systems used in this work. Subsequent discussion is organized around efficiency, selectivity, and system retention, which are represented in Equation [15] by the first, second, and last two terms, respectively.

efficiency

Sources of band dispersion in MECC have been studied extensively (32, 94, 95). The ultimate limit of efficiency in all forms of CE is axial diffusion. However, resistance to mass transfer (the association-dissociation of solutes with micelles or CDs and

mass transport between micelles or CDs) can be an important source of band dispersion in capillary electrokinetic chromatography. The fact that micelles and charged CDs are polydisperse can exacerbate problems with slow mass transfer. The problem in MECC is lessened by the fact that normal micelles are dynamic assemblies and are rapidly exchanging with free surfactant. Conversely, the CMβ-CD used in this work contains a complex mixture of CDs derivatized to varying degrees and at various hydroxyl positions (21 such hydroxyl positions exist on β-CD) (34). The manufacturer quotes an average of 3 CM per β-CD. However, our mass spectral investigation of this CD indicated a wide distribution in the degree of substitution. Thus, rapid association-dissociation kinetics and transport between CDs is expected to be very important in achieving high efficiency.

Figure 19 reveals that efficiency in CDCE can be comparable to MECC. The efficiencies for the pyrene peaks in that figure are 210,000 plates/m for the MECC case and 150,000 and 220,000 plates/m for the CDCE cases that employ β-CD and HPβ-CD, respectively, as the neutral CD. The effective diffusion coefficients of the solutes in the CDCE separations should be very low since they are associated with bulky CD molecules. Thus, the observed efficiency is probably too low for axial diffusion to be a significant source of dispersion.

The concentration of CD can be important in providing high efficiency as demonstrated in Figure 20. BaP and chrysene are unresolved with the simple CDCE system employed and thus shown separately in the figure. When the CD concentrations are increased

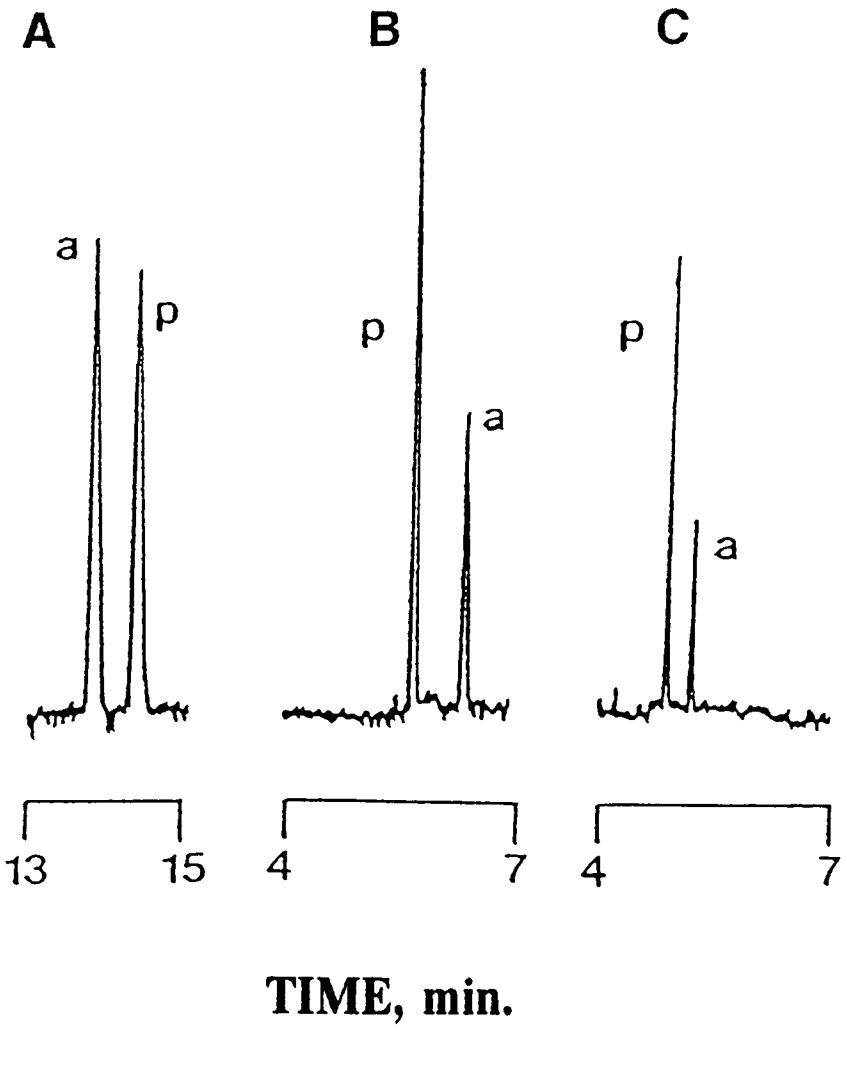

Figure 19 Separations of anthracene (a) and pyrene (p). Conditions: **A)** 50 mM SDS. **B)** 5 mM β-CD:10 mM CMβ-CD. **C)** 5 mM HPβ-CD:10 mM CMβ-CD. All mobile phases were pH 6 and contained 20 % ACN.

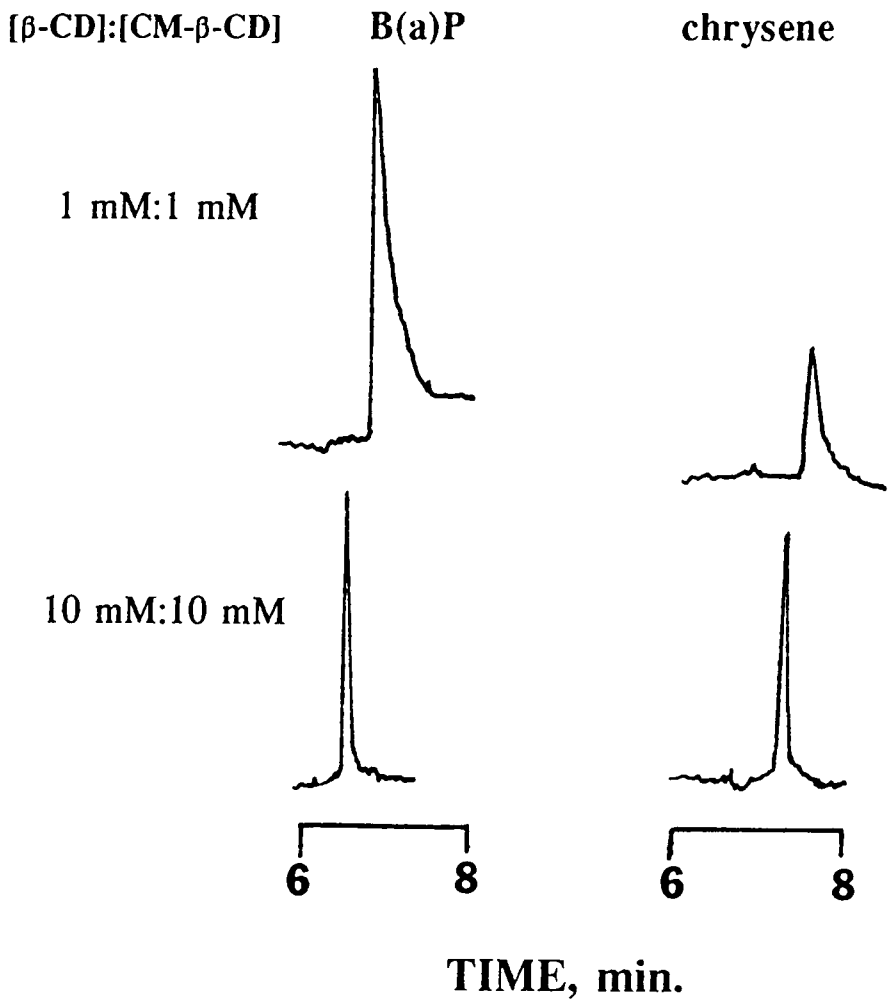

Figure 20 CDCE peak profiles for BaP and chrysene at low and high CD concentrations. Conditions: mobile phases were pH 6 and contained 30 % MeOH.

from 1 to 10 mM, efficiency is improved dramatically. A possible increase in temperature, due to a greater thermal load, and improved solubility may contribute to the observed efficiency effect. However, running currents and PAH concentrations were fairly low in that experiment. It is more likely that improved mass transfer is responsible for the superior efficiency at the higher CD concentration. Since the PAHs are essentially insoluble in the aqueous phase, CDs must get very close in order to exchange solute. The average inter-CD distance is small for both systems (22 nm and 8 nm for the small and large CD concentrations, respectively). Thus, the frequency of CD encounters is extremely high in each system and should not prohibit mass transfer. However, the better proximity of CDs for the high concentration case could influence the orientation for solute exchange between CDs and/or the association-dissociation kinetics. In any event, increases in CD concentration can improve efficiency, but were limited in this work to CMβ-CD concentration less than about 15 mM due to the onset of thermal dispersion.

In some runs, the current was observed to increase. In those cases the flow rate appeared to change and peaks exhibited severe tailing. This indicates interaction between the CD phase and the capillary wall. Given the like charges of the silica surface and the CMβ-CD, this is somewhat surprising. In most cases, a base (10 mM NaOH) rinse restored separation performance.

selectivity

The unique selectivity afforded by the CDCE technique is evidenced by a reversal of elution order, relative to MECC, of pyrene and anthracene in Figure 19. The CDCE system used for Figure 19B involves native and charged β-CD. If the CM derivatization did not alter the complexation characteristics of the β-CD, there would be no separation of these PAHs even though they have very different complexation constants. In fact, K_D values would be expected to be the same for all compounds. Obviously, the derivatization of β-CD with CM in this particular commercial product, strongly enhances the inclusion complexation with anthracene relative to pyrene. Since dozens of derivatized CDs are commercially available, CDCE systems with diverse selectivities should be possible.

Another illustration of unique selectivity is shown in Figure 21. It is intriguing that the elution order for the CDCE separation is pyrene (four fused benzene rings), BaP (five rings), chrysene (four rings), and anthracene (three rings). Unlike micellar systems, which can form mixed micelles when multiple surfactants are used, and may interact with the CD when CD-MECC is performed, the CDs in the CDCE technique act independently. Thus, complex systems can be designed in CDCE with predictable effects on selectivity. For example, in order to resolve BaP and chrysene (see Figure 21B) it was necessary to employ a ternary CD system that contained a low concentration of γ-CD; prior work had revealed a strong association between BaP and γ-CD (71).

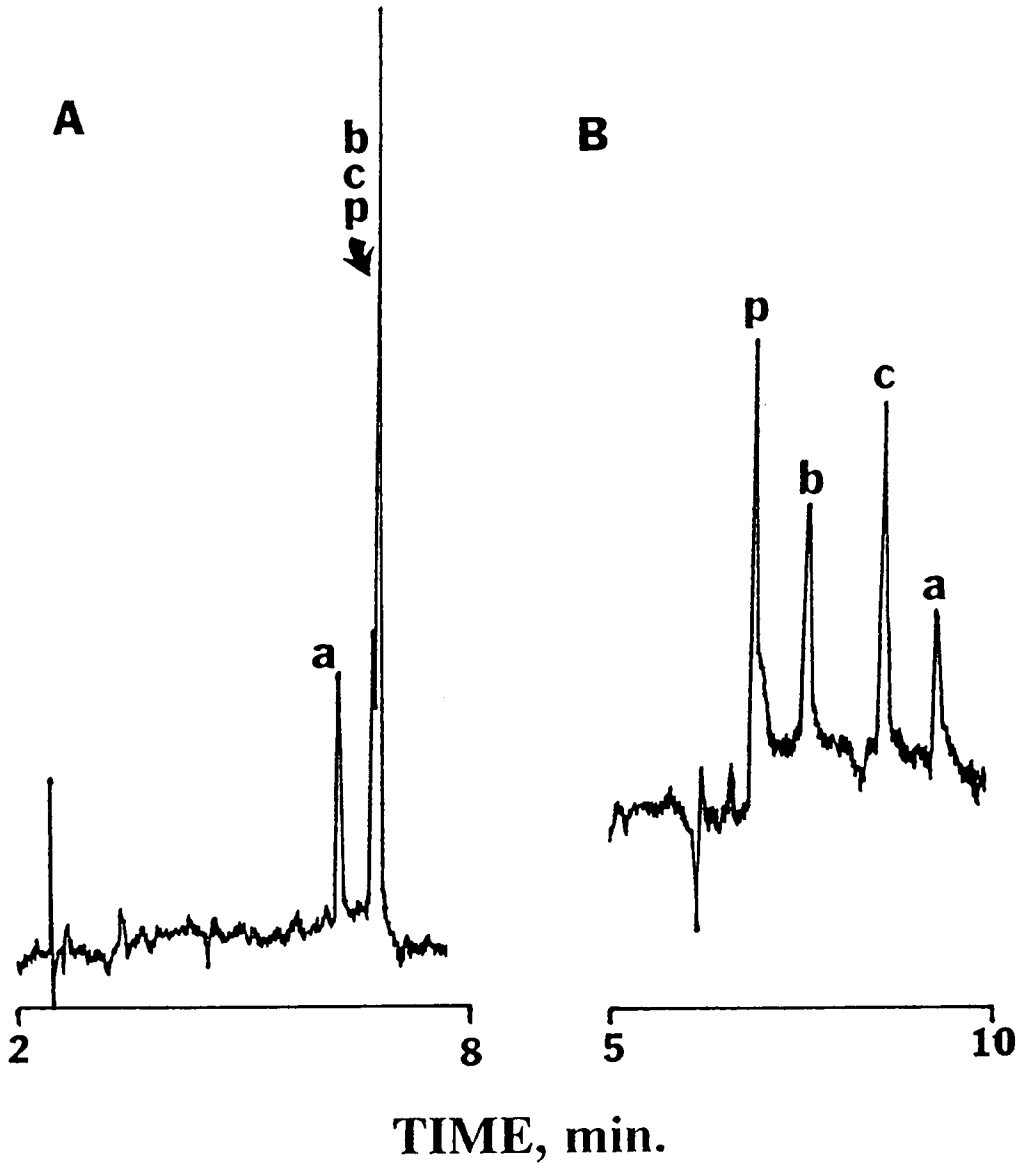

Figure 21 Separations of several PAHs by CD-MECC and CDCE. Solutes and conditions: anthracene (a), pyrene (p), chrysene (c), and BaP (b). **A)** 50 mM SDS, 8 mM γ-CD, 8 mM β-CD. **B)** 8 mM β-CD & 1 mM γ-CD:10 mM CMβ-CD with 30 % MeOH.

system retention

Optimum capacity factor for the MECC technique depends on the width of the elution window and generally falls in the range of 1-5 (31). Hydrophobic molecules exhibit excessive k' values and tend to co-elute near the end of the window. Thus, it is possible to improve R_s without improving selectivity by simply reducing k' and/or extending the elution window. The elution window in CDCE is defined by t_{ne} and t_{ch} and, as such, depends on electroosmotic flow and the electrophoretic mobility of the charged CD. Low electroosmotic flow and a high degree of CMβ-CD substitution favor a wide elution window, but can result in long separation time and influence CD inclusion. Because t_{ch} is not well-defined in CDCE (see above), the width of the elution window is also not well-defined. In fact, since substitution of the CD is shown in this work to influence solute/CD inclusion, it is possible for compounds with different distributions in their affinities for the CMβ-CD "mixture" to experience different effective windows under the same set of operating conditions. In general, the windows for the CDCE systems investigated in this work are smaller than in MECC. This can be seen from an inspection of Figure 21.

Table VIII presents the effects of organic modifier (MeOH) and pH on the retention times of pyrene and anthracene, which elute near the beginning and the end of the window, respectively. As the % of MeOH is increased, the electroosmotic flow decreases and the spacing between the compounds increases. It is possible that an increase in the solubility of anthracene in the high organic content

separation buffer may partially mask the extension of the window. This illustrates both the influence of the width of the elution window on resolution and the ability of the CDCE technique to tolerate high concentrations of organic solvents. Table VIII also demonstrates a pH-related increase in the width of the window, due to a reduction in electroosmotic flow as pH is decreased, and the eventual collapse of the window as the charged CD phase is neutralized.

Because of its strong influence on R_s, it would be desirable to exert close control over k' in capillary electrokinetic chromatography. This is easily accomplished in CDCE. Equation [16] illustrates the relationship between k' and CD phase ratio. This equation assumes no direct interaction between the solutes and the separation buffer. Since $V_{charged}/V_{neutral}$ is proportional (and roughly equal to) to [CMβ-CD]/[β-CD], a plot of concentration ratio versus k' should be linear with a slope approximately equal to the distribution coefficient. Plots for anthracene and pyrene are presented in Figure 22. Phase ratio is approximated by CD concentration ratio. CMβ-CD concentration was held constant at 5 mM and β-CD concentration was changed from 0 to 10 mM. The no β-CD case, with an injection of anthracene, was used to establish t_{ch} and solvent disturbances were used to mark t_{ne}. The plots are reasonably linear and the K_D values are consistent with the stronger association of anthracene with CMβ-CD.

Table VIII. Effect of organic modifier and pH on CDCE system retention.

	t_{pyrene} (min)	$t_{anthracene}$ (min)	Δt (min)
Organic modifier			
a + 1% MeOH	6.3	8.1	1.8
a + 20% MeOH	6.8	9.1	2.3
a + 30% MeOH	12.5	15.5	3.0
a + 40% MeOH	15.3	18.8	3.5
pH			
b at pH 6.4	5.1	6.60	1.5
b at pH 3.3	9.1	14.5	5.4
b at pH 2.5	10.6	10.6	0

a) Mobile phase with 8 mM β-CD, 1 mM γ-CD:10 mM CMβ-CD.
b) Mobile phase with 5 mM β-CD:10 mM CMβ-CD.

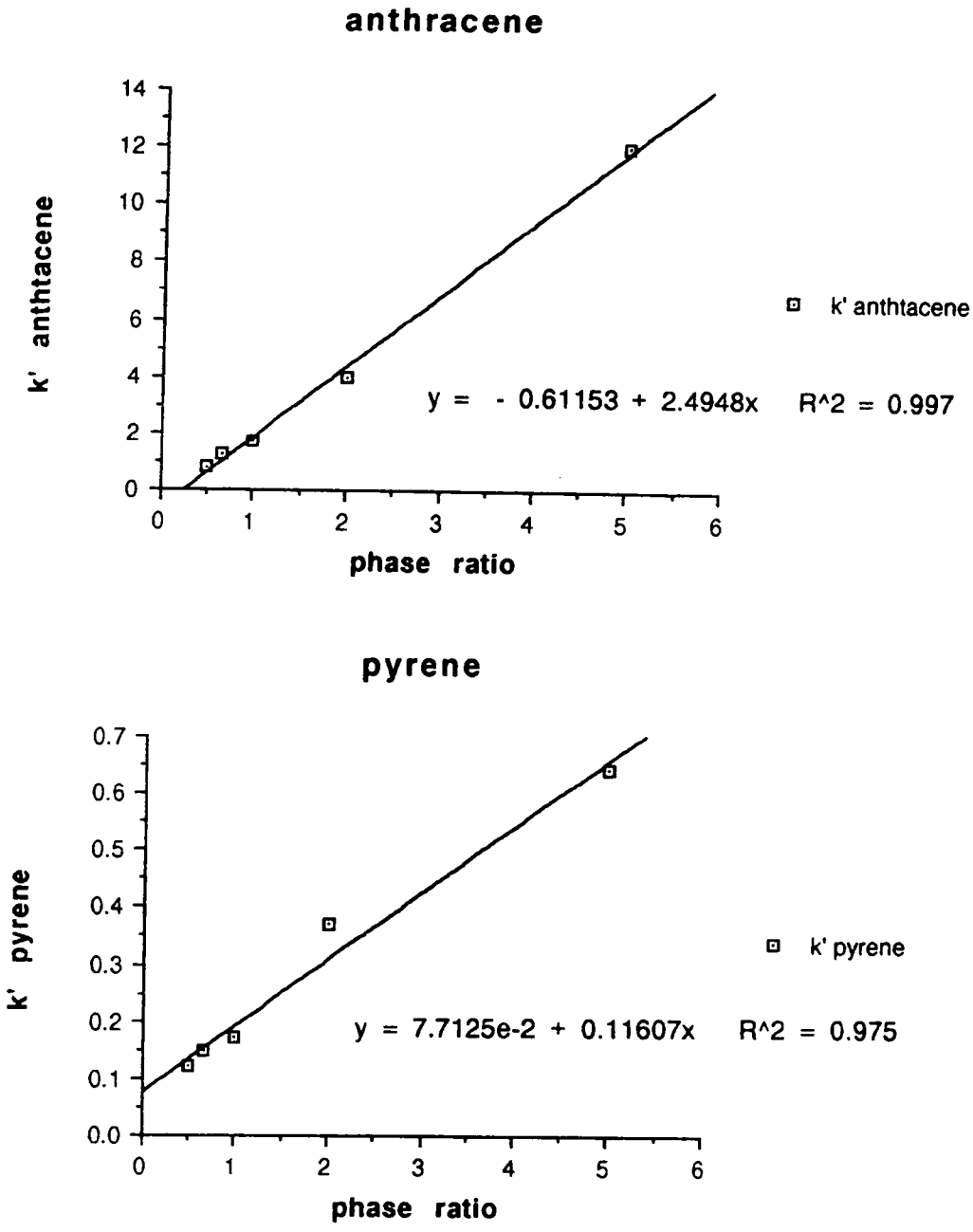

Figure 22 Plots of phase ratio (approximated as concentration ratio [CMβ-CD] / [β-CD]) versus approximate k'.

In summary, the dual CD variant of capillary electrokinetic chromatography described in this chapter adds new versatility to CE. While it resembles MECC in many regards, it provides unique selectivity and should be particularly useful in isomeric separations, where the geometrical and chiral characteristics of CD inclusion can be exploited. Convenient control over k', and the ability to employ complex CD systems and high concentrations of organic solvents, represent other desirable traits of this approach.

Chapter 10
Concluding Remarks

The use of CE as a high efficiency separation method is growing rapidly. Even with the limited experience of this author, it is evident that studies of the "obvious" aspects of CE have been exhausted. This has left researchers to explore very specialized, and often experimentally difficult areas of the technique such as those described in this dissertation.

Very generally, the goals of this research were to employ CD additives in CE separations and to elucidate the mechanisms by which these separations occurred using molecular modeling. The attainment of these goals is evident in the discussions of three modes of CE separations found in the preceding chapters.

The strength of CD-MECC was demonstrated in separations of highly hydrophobic PAH compounds. The ease of optimization of k' values through adjustment of type and concentration of surfactant and organic solvent was presented. Furthermore, several types of neutral CDs were shown to provide the selectivity necessary to resolve various sized PAHs. Perhaps most impressive was the use of CD-MECC to separate two types of BaP isomers. Such separations, which had not been reported previously, highlight the strength of CDs as highly selective mobile phase additives.

The mechanism of the BaP isomer separations mentioned above was determined to be one of direct mass transfer of the BaP isomer between an SDS micelle and a γ-CD molecule. The interaction of

each BaP isomer with the SDS micelles should be nearly equal as their hydrophobicities are similar. For this reason, interactions between each isomer and a γ-CD molecule were studied to confirm the elution order observed. Reasonable correlations between separation behavior and computationally derived interaction energies were drawn. Even though only three orientations and two dimensional positioning were considered in this work, it was shown that molecular modeling techniques can provide insights into pertinent retention mechanisms.

The second technique described, CD-CE, is most commonly used in enantiomeric separations. In this work, CD-CE was shown to be a successful alternative to previously reported methods of separating enantiomers of several DNS-amino acids and binaphthyl compounds. In all cases, it was found that there exists an optimum CD concentration that leads to maximum enantiomeric resolution. Just as importantly, it was determined that the effects of separation conditions on general elution behavior must be considered or separated enantiomer pairs will co-elute with other enantiomers.

A statistical mechanical approach to treating enantiomer/CD interaction energies derived from molecular modeling studies provided reasonable correlations with CD-CE separation performance. Interestingly enough, these correlations were drawn in two different ways depending on the structural characteristics of the solutes. In the BN study, correlations were found when the behavior of individual BN compounds in the presence of each different CD was examined. However, correlations were found when

the separation behavior of a series of amino acid enantiomers with one type of CD was considered. This was an important finding with regard to using molecular modeling as a tool for predicting enantiomeric separation behavior.

CDCE was the third technique studied. Prior to our studies, the simultaneous use of neutral and charged CDs in CE separations of water insoluble PAH molecules had not been reported. For this reason, these initial results were presented with a focus on fundamental parameters such as efficiency, selectivity, and system retention.

Of these CDCE parameters, selectivity can be altered most significantly giving rise to unique elution orders. Many types of derivatized (neutral and charged) CDs having various degrees of substitution are commercially available, providing a wealth of separation possibilities.

Molecular modeling studies of solute/CD interactions could greatly reduce analysis time by allowing one to predict which combinations of CDs are appropriate to separate the solutes of interest. Such studies are the current focus of research by this author.

In closing, it can be said that CDs are a powerful class of separation buffer additives in CE separations of chiral and non-chiral compounds. Further research in this area will most likely focus on the use of very specialized (with regard to type and number of substitutions) CD derivatives to form very specific inclusion complexes with solutes. Throughout this work, molecular modeling

was shown to provide answers to some fundamental questions regarding solute/CD interactions but its limitations are still glaringly obvious. With improvements in computer software and hardware, one can only imagine the information that will be available without even filling a capillary with separation buffer. Perhaps eventually, molecular modeling will be used to predict, rather than just explain, CE separation behavior.

References

References

(1) McNair, H. M.; Bonelli, E. J. *Basic Gas Chromatography*; Consolidated Printers: Berkeley, 1968, Ch. 1.

(2) Poole, C. F.; Poole, S. K. *Chromatography Today*, Elsevier Science Publishing Co., Inc.: New York, 1991, pp. 106-107 and 312-313.

(3) Johnson, E. L.; Stevenson, R. *Basic Liquid Chromatography*, Consolidated Printers: Berkeley, CA, 1978, Ch. 1.

(4) Karger, B. L.; Foret, F. In *Capillary Eletrophoresis Technology*; Guzman, N. A., Ed.; Marcel Dekker, Inc.: New York, 1993, Ch. 1.

(5) Hjerten, S. *Chromatogr.Rev.* **1967**, *9*, 122.

(6) Catsimpoolas, N. *Sep. Sci.* **1971**, *6*, 435.

(7) Virtanen, R. *Acta Polytech. Scand. Appl. Phys. Seer.* **1974**, 123.

(8) Mikkers, F. E.; Evaraerts, F. M.; Verheggen, T. *J. Chromatogr.* **1979**, *169*, 11.

(9) Jorgenson, J.; Lukacs, K. D. *Anal. Chem.* **1981**, *53*, 1298.

(10) Kuhr, W. In *Capillary Electrophoresis: Theory and Practice*, Camilleri, P., Ed.; CRC Press: Boca Raton, 1993, Ch. 3.

(11) Grossman, P. D. In *Capillary Electrophoresis: Theory and Practice*, Grossman, P. D., Colburn, J. C., Eds.; Academic Press, Inc.: New York, 1992, Ch. 1.

(12) Monnig, C. A.; Kennedy, R. T. *Anal. Chem.* **1994**, *66*, 280R.

(13) Marina, M. L.; Torre, M. *Talanta* **1994**, *41*, 1411.

(14) Bereuter, T. L. *LC-GC* **1994**, *12*, 748.

(15) Ward, T. *Anal. Chem.* **1994**, *66*, 633A.

(16) Novotony, M.; Soini, H.; Stefansson, M. *Anal. Chem.* **1994**, *66*, 646A.

(17) Vespalec, R.; Bocek, P. *Electrophoresis* **1994**, *15*, 755.

(18) Balchunas, A. T.; Sepaniak, M. J. *Anal. Chem.* **1987**, *59*, 1466.

(19) Clark, B. K.; Nickles, C.; Morton, K; Sepaniak, M. J. *J. Microcol. Sep.* **1994**, *6*, 503.

(20) Sepaniak, M. J.; Powell, A. C.; Swaile, D. F.; Cole, R. O. In *Capillary Electrophoresis: Theory and Practice*, Grossman, P. D., Colburn, J. C., Eds.; Academic Press, Inc.: New York, 1992, Ch. 6.

(21) Copper, C. L.; Staller, T. D.; Sepaniak, M. J. *Poly. Arom. Compds.* **1993**, *3*, 121.

(22) Sepaniak, M. J.; Copper, C. L.; Whitaker, K. W.; Anigbogu, V. C. *Anal. Chem.* **1995**, 67, 2037.

(23) Otsuka, K.; Terabe, S. *J. Chromatogr.* **1990**, *515*, 221.

(24) Cole, R. O.; Sepaniak, M. J.; Hinze, W. L. *J. High Res. Chromatogr.* **1990**, *13*, 579.

(25) Copper, C. L.; Davis, J. B.; Cole, R. O.; Sepaniak, M. J. *Electrophoresis* **1994**, *15*, 785.

(26) Sepaniak, M. J.; Cole, R. O.; Clark, B. K. *J. Liq. Chromatogr.* **1992**, *15*, 1023.

(27) Gozel, P.; Gassmann, E.; Michelsen, H.; Zare, R. N. *Anal. Chem.* **1987**, *59*, 44.

(28) Kuhn, R.; Erni, F.; Bereuter, T.; Hausler, J. *Anal. Chem.* **1992**, *64*, 2815.

(29) Armstrong, D. W.; Rundlett, K.; Reid, G. L. *Anal. Chem.* **1994**, *66*, 1690.

(30) Valtcheva, L.; Mohammad, J.; Pettersson, G.; Hjerten, S. *J. Chromatogr.* **1993**, *638*, 263.

(31) Terabe, S.; Otsuka, K.; Ando, T. *Anal. Chem.* **1985**, *57*, 834.

(32) Sepaniak, M. J.; Cole, R. O. *Anal. Chem.* **1987**, *59*, 472.

(33) Terabe, S.; Otsuka, K.; Ichikawa, K.; Tsuchiya, A.; Ando, T. *Anal. Chem.* **1984**, *56*, 111.

(34) Stratten, C. *Biopharm* **1991**, *4*, 44.

(35) Szejtli, J. *Cyclodextrins and Their Inclusion Complexes*; Akademiai Kiado: Budapest, 1978.

(36) Bender, M. L.; Komiyama, M. *Cyclodextrin Chemistry;* Springer-Verlag: Berlin, 1978.

(37) Saunders, M.; Jarret, R. M. *J. Comput. Chem.* **1986**, *7*, 578.

(38) Boyd, D. B. In *Reviews in Computational Chemistry*, Lipkowitz, K. B.; Boyd, D. B., Eds.; VCH Publishers: New York, 1990, Ch. 9.

(39) Berkert, U.; Allinger, N. L. *Molecular Mechanics*, ACS Monograph No. 177, 1982.

(40) Boyd, D. B.; Lipkowitz, K. B. *J. Chem. Educ.* **1982**, *59*, 269.

(41) Rasmussen, K. In *Lecture Notes in Chemistry*, Vol. 27, Berthier, G., Ed.; Springer-Verlag: Berlin, 1985.

(42) Allinger, N. L.; Lii, J. H. *J. Comput. Chem.* **1987**, *8*, 1146.

(43) Lipkowitz, K. B. In *Conformational Analysis of Cyclohexanes, Cyclohexadienes, and Related Hydroaromatic Compounds*, Ravideau, P. W., Ed.; VCH Publishers: New York, 1989, p. 299.

(44) Cohen, N. C.; Blaney, J. M.; Humblet, C.; Gund, P.; Barry, D. C. *J. Med. Chem.* **1990**, *33*, 883.

(45) Lipkowitz, K. B.; Antell, S.; Baker, B. *J. Org. Chem.* **1989**, *54*, 5449.

(46) Lipkowitz, K. B.; Baker, B. *Anal. Chem.* **1990**, *62*, 770.

(47) Lipkowitz, K. B.; Demeter, D. A.; Zegarra, R.; Larter, R.; Darden, T. *J. Am. Chem. Soc.* **1988**, *110*, 3446.

(48) Lipkowitz, K. B.; Baker, B.; Zegarra, R. *J. Comput. Chem.* **1989**, *10*, 718.

(49) Lipkowitz, K. B.; Demeter, D. A.; Parish, C. A.; Landwer, J. M. *J. Comput. Chem.* **1987**, *8*, 753.

(50) Lipkowitz, K. B.; Green, K.; Yang, J. *Chirality* **1992**, *4*, 205.

(51) Lipkowitz, K. B. *J. Org. Chem.* **1991**, *56*, 6357.

(52) Lipkowitz, K. B.; Green, K.; Yang, J.; Pearl, G.; Peterson, M. A. *Chirality* **1993**, *5*, 51.

(53) Lu, T. X.; Zhang, D. B.; Dong, S. *J. Chem. Soc. Faraday Trans. 2* **1989**, *85*, 1439.

(54) Kostense, A. S.; Van Helden, S. Pl; Janssen, L. H. *J. Comput.-Aided Mol. Des.* **1991**, *5*, 525.

(55) Lipkowitz, K. B.; Raghothama, S.; Yang, J. *J. Am. Chem. Soc.* **1992**, *114*, 1554.

(56) Camilleri, P.; Murphy, J. A.; Saunders, M. R.; Thorpe, C. J. *J. Comput.-Aided Mol. Des.* **1991**, *5*, 277.

(57) Arnold, E. N.; Lillie, T. S.; Beesley, T. E. *J. Liq. Chromatogr.* **1989**, *12*, 337.

(58) Studt, T. *R & D Magazine*, **1995**, *February*, 77.

(59) Staller, T. D. "Novel Detection Alternatives for Capillary Electrokinetic Separations" Doctor of Philosophy Dissertation, The University of Tennessee, 1995.

(60) Product Literature: Evans and Sutherland Workstation, pp. 2.1-2.7.

(61) Bjorseth, A.; Ramdahl, T. In *Handbook of Polycyclic Aromatic Hydrocarbons, Vol. 2*, Bjorseth, A., Ramdahl, T., Eds.; Marcel Dekker, Inc.: New York, 1985, Ch. 1.

(62) Bartle, K. D. In *Handbook of Polycyclic Aromatic Hydrocarbons, Vol. 2*, Bjorseth, A., Ramdahl, T., Eds.; Marcel Dekker, Inc.: New York, 1985, Ch. 6.

(63) Wise, S. A. In *Handbook of Polycyclic Aromatic Hydrocarbons, Vol. 1*, Bjorseth, A., Ed.; Marcel Dekker, Inc.: New York, 1983, Ch. 5.

(64) Hirata, Y.; Novotny, M. *J. Chromatogr.* **1980**, *186*, 521.

(65) Ishii, D.; Tsuda, T.; Hibi, K; Takevchi, T.; Nakanishi, T. *J. High Res. Chromatogr. Chromatogr. Commun.* **1979**, *2*, 372.

(66) Hirata, Y.; Novotny, M.; Tsuda, T.; Ishii, D. *Anal. Chem.* **1979**, *51*, 1807.

(67) Balchunas, A. T.; Capacci, M.; Sepaniak, M. J.; Maskarinec, M. P. *J. Chromatogr. Sci.* **1985**, *23*, 381.

(68) Wehry, E. L. In *Handbook of Polycyclic Aromatic Hydrocarbons, Vol. 1*, Bjorseth, A., Ed., Marcel Dekker, Inc.: New York, 1983, Ch. 8.

(69) Cole, R. O.; Sepaniak, M. J.; Hinze, W. L.; Gorse, J.; Oldiges, K. *J. Chromatogr.* **1991**, *557*, 113.

(70) Gorse, J.; Balchunas, A. T., Swaile, D. F.; Sepaniak, M. J. *J. High Res. Chromatogr.Chromatogr. Commun.* **1988**, *11*, 554.

(71) Copper, C. L.; Sepaniak, M. J. *Anal.Chem.* **1994**, *66*, 147.

(72) Shimada, K.; Komine, Y.; Mitamura, K. *J. Chromatogr. Sci.* **1990**, *28*, 53.

(73) Terabe, S.; Miyashita, Y.; Shibata, O.; Barnhart, E. R.; Alexander, L. R.; Patterson, D. G.; Karger, B. L.; Hosoya, K.; Tanaka, N. *J. Chromatogr.* **1990**, *516*, 23.

(74) Nishi, H.; Fukuyama, T.; Terabe, S. *J. Chromatogr.* **1991**, *553*, 503.

(75) Ong, C. P.; Ng, C. L.; Lee, H. K.; Li, S. F. *J. Chromatogr.* **1991**, *547*, 419.

(76) Shimada, K.; Yoshihiro, K.; Oe, T. *J. Liq. Chromatogr.* **1989**, *12*, 491.

(77) Issaq, H. J.; Glennon, M. L.; Weiss, D. E.; Fox, S. D. In *Ordered Media in Chemical Separations*, Hinze, W. L.; Armstrong, D. W., Eds.; American Chemical Society: Washington, D.C., 1987, Ch. 15.

(78) Komatsu, N.; Hashizume, M.; Sugita, T.; Uemura, S. *J. Org. Chem.* **1993**, *58*, 4529.

(79) Chong, J. M.; MacDonald, G. K.; Park, S. B.; Wilkinson, S. H. *J. Org. Chem.* **1993**, *58*, 1266.

(80) Marvoka, K.; Murase, N.; Yamamoto, H. *J. Org. Chem.* **1993**, *58*, 2938.

(81) Hu, W.; Takeuchi, T.; Haraguchi, H. *Chromatographia* **1992**, *33*, 63.

(82) Hu, W.; Takeuchi, T.; Haraguchi, H. *J. High Res. Chromatogr.* **1992**, *15*, 275.

(83) Hu, W.; Takeuchi, T.; Haraguchi, H. *Chromatographia* **1992**, *33*, 58.

(84) Stalcup, A. M.; Jin, H. L.; Armstrong, D. W. *J. Liq. Chromatogr.* **1990**, *13*, 473.

(85) Wren, S. A.; Rowe, R. C. *J. Chromatogr.* **1992**, *603*, 235.

(86) Wren, S. A. *J. Chromatogr.* **1993**, *636*, 57.

(87) Kuhn, R.; Hoffstetter-Kuhn, S. *Chromatographia* **1992**, *34*, 505.

(88) Powell, A. C.; Sepaniak, M. J. *Anal. Instrum.* **1993**, *21*, 25.

(89) Sepaniak, M. J.; Swaile, D. F.; Powell, A. C. *J. Chromatogr.* **1989**, *480*, 185.

(90) Terabe, S.; Ozaki, K.; Otsuka, K.; Ando, T. *J. Chromatogr.* **1985**, *332*, 211.

(91) Schmitt, T.; Engelhardt, H. *Chromatographia* **1993**, *37*, 475.

(92) Smith, N. *J. Chromatogr.* **1993**, *652*, 259.

(93) Nardi, A.; Eliseev, A.; Bocek, P.; Fanali, S. *J. Chromatogr.* **1993**, *638*, 247.

(94) Terabe, S.; Otsuka, K.; Ando, T. *Anal. Chem.* **1989**, *61*, 251.

(95) Davis, J. M. *Anal. Chem.* **1989**, *61*, 2455.

(96) Anigbogu, V. C.; Copper, C. L.; Sepaniak, M. J. *J. Chromatogr.* **1995**, in press.

Appendix

Structures of Solute Molecules

Structures of Polycyclic Aromatic Hydrocarbons

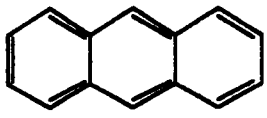

Anthracene

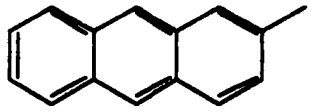

2-Methylanthracene

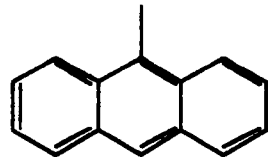

9-Methylanthracene

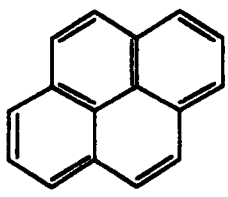

Pyrene

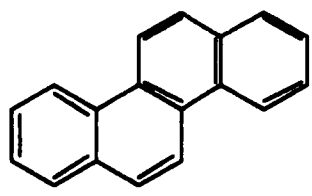

Chrysene

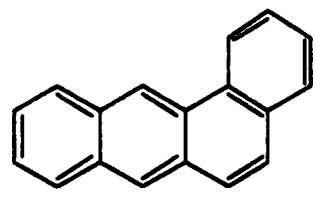

Benz(a)anthracene

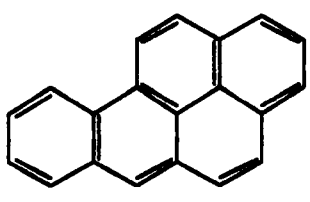

Benzo(a)pyrene

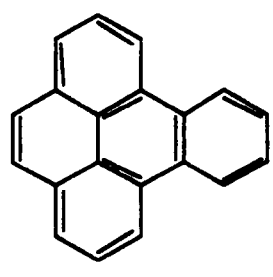

Benzo(e)pyrene

Structures of DNS-Amino Acids

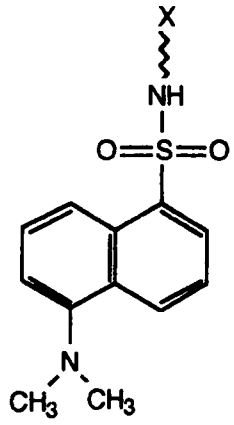

5-Dimethylamino-1-naphthalene sulfonyl group

Where X =

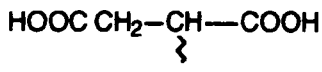

Aspartic Acid

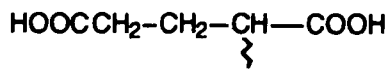

Glutamic Acid

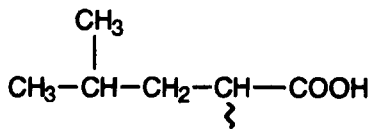

Leucine

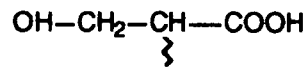

Serine

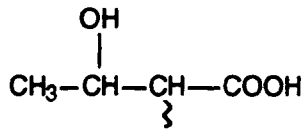

Threonine

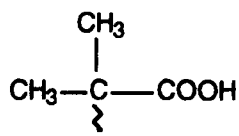

Valine

Vita

Christine Leigh Copper was born in Camden, New Jersey on November 18, 1969 and soon moved to Worcester, Pennsylvania. Upon graduation from Methacton High School in June of 1987, she entered Mary Washington College in Fredericksburg, Virginia where she was a Regional Scholar and a member of two national championship tennis teams. She received a Bachelor of Science degree, with honors in chemistry, in May of 1991. In August of that same year, she entered the University of Tennessee, Knoxville and successfully completed the requirements for a Doctor of Philosophy degree in chemistry in the summer of 1995. She has accepted a position as an assistant professor of chemistry at the United States Naval Academy in Annapolis, Maryland.